# Molecular Dynamics and Static Solvation Studies of Amiloride

**Ronald A. Buono,[†] Thomas J. Venanzi,[‡] Randy J. Zauhar,[§] Victor B. Luzhkov,[†,∥] and Carol A. Venanzi*[,†]**

*Contribution from the Department of Chemical Engineering, Chemistry, and Environmental Science, New Jersey Institute of Technology, Newark, New Jersey 07102, Chemistry Department, College of New Rochelle, New Rochelle, New York 10805, and Biotechnology Institute and Department of Molecular and Cell Biology, 519 Wartik Laboratory, The Pennsylvania State University, University Park, Pennsylvania 16802*

*Received July 9, 1993*[⊕]

**Abstract:** The GROMOS molecular mechanics and dynamics force field was extended and modified in order to investigate the static and dynamic conformational properties of amiloride conformers in solution. Torsional potential functions, Lennard–Jones parameters, and atomic point charges were derived for the free base and protonated species of amiloride. The effect of solvent on the conformation, energy, and intramolecular hydrogen bonding patterns of the free base (A1 and A4) and protonated (F1) species of amiloride was examined by 25-ps simulations of each species in a bath of SPC water molecules. The large torsional barriers for A1 to A4 and F1 to F4 conversion, determined from 3-21G* molecular orbital calculations, were found to constrain the average structure of each species to a nearly-planar conformation. This suggests that amiloride binds to the ion channel in a planar conformation. In agreement with previous *ab initio* calculations, the molecular dynamics simulations found the relative internal energy of the A1 conformer to be lower than that of A4. However, the solute–solvent interaction energy was lower for A4 than A1, consistent with the larger dipole moment of A4. Combined, these trends still predict the A1 conformer to be more stable in solution than A4. Static solvation studies of amiloride with an induced polarization charge boundary element (IPCBE) continuum solvent method, the Langevin dipole method, and the self-consistent reaction field method gave qualitatively similar results. These results help to clarify the NMR studies of Smith et al. (*J. Am. Chem. Soc.* **1979**, *101*, 191), who were unable to distinguish between the A1 and A4 conformers in solution. Calculation of the electrostatic contribution to both the relative hydration enthalpy and the relative hydration free energy of amiloride conformers using the IPCBE method showed that the maximum difference in these quantities is about 4%.

## Introduction

Nonspecific solute–solvent interactions may influence solute molecular conformation and reactivity. In the last 30 years, several continuum, microscopic, and empirical solvation models have been developed to include the effect of solvent in quantum chemical and empirical force field calculations. The classical description of solutes in a continuous medium (reaction field) by Born,[1] Kirkwood,[2] and Onsanger[3] forms the foundation of the continuum approaches. Drummond[4] has reviewed the development of several continuum, point charge, and hybrid models used in quantum chemical calculations, and Tapia[5] has described the theoretical formalism that relates five different continuum models. Reaction field models have been applied to the calculation of a wide range of problems using semiempirical[6–10] and *ab initio*[11,12] molecular orbital theory, free energy perturbation theory,[13] and molecular mechanics minimization.[14d] Microscopic models involve the use of discrete solvent molecules, as in molecular dynamics (MD) or Monte Carlo simulations, or are based on approximations such as the Langevin dipole[15] (LD) model, which treats the solvent molecules as polarizable point dipoles. Despite this simplified treatment, the LD method has proven to be useful in the study of solvent effects and gives reliable estimates of the solvation energies of small molecules and proteins.[15] Empirical solvation models[16,17] depend on the solvent accessible surface area of the solute and differ in atom classification and attributes. Several

* Author to whom correspondence should be addressed.
† New Jersey Institute of Technology.
‡ College of New Rochelle.
§ The Pennsylvania State University.
∥ Permanent address: Institute of Chemical Physics, Chernogolovka, Moscow Region, Russia 142432.

⊕ Abstract published in *Advance ACS Abstracts*, January 15, 1994.

(1) Born, M. *Z. Phys.* **1920**, *1*, 45.
(2) Kirkwood, J. G. *J. Chem. Phys.* **1934**, *2*, 351.
(3) Onsanger, L. *J. Am. Chem. Soc.* **1936**, *58*, 1486.
(4) Drummond, M. *Prog. Biophys. Mol. Biol.* **1986**, *47*, 1.
(5) Tapia, O. In *Quantum Theory of Chemical Reactions, Vol. II*; Daudel, R., Pullman, A., Salem, L., Veillard, A., Eds.; D. Reidel: Dordrecht, The Netherlands, 1980; pp 25–72.
(6) Szafran, M.; Karelson, M. M.; Katritzky, A. R.; Koput, J.; Zerner, M. C. *J. Comput. Chem.* **1993**, *14*, 371.
(7) (a) Wang, B.; Ford, J. P. *J. Chem. Phys.* **1992**, *97*, 4162. (b) Ford, G. P.; Wang, B. *J. Am. Chem. Soc.* **1992**, *114*, 10563.
(8) (a) Cramer, C. J.; Truhlar, D. G. *J. Am. Chem. Soc.* **1991**, *113*, 8552. (b) Cramer, C. J.; Truhlar, D. G. *J. Am. Chem. Soc.* **1991**, *113*, 8305. (c) Cramer, C. J.; Truhlar, D. G. *Science* **1992**, *256*, 213. (d) Cramer, C. J.; Truhlar, D. G. *J. Am. Chem. Soc.* **1992**, *114*, 8795. (e) Urban, J. J.; Truhlar, D. G. *J. Comput. Chem.* **1992**, *13*, 1089. (f) Urban, J. J.; Cramer, C. J.; Famini, G. R. *J. Am. Chem. Soc.* **1992**, *114*, 8226. (g) Cramer, C. J.; Truhlar, D. G. *J. Am. Chem. Soc.* **1993**, *115*, 8810.
(9) Furuki, T.; Sakurai, M.; Inoue, Y.; Chûjô, R.; Harata, K. *Chem. Phys. Lett.* **1992**, *188*, 584.
(10) Alkorta, I.; Villar, H. O.; Perez, J. J. *J. Comput. Chem.* **1993**, *14*, 620.
(11) (a) Bonaccorsi, R.; Cimiraglia, R.; Tomasi, J. *J. Chem. Phys. Lett.* **1983**, *99*, 77. (b) Bonaccorsi, R.; Cimiraglia, R.; Tomasi, J.; Miertuš, S. *J. Mol. Struct. (THEOCHEM)* **1983**, *94*, 11.
(12) (a) Wong, M. W.; Wiberg, K. B.; Frisch, M. *J. Chem. Phys.* **1991**, *95*, 8991. (b) Wong, M. W.; Frisch, M. J.; Wiberg, K. B. *J. Am. Chem. Soc.* **1991**, *113*, 4776. (c) Wong, M. W.; Wiberg, K. B.; Frisch, M. J. *J. Am. Chem. Soc.* **1992**, *114*, 523. (d) Wong, M. W.; Wiberg, K. B.; Frisch, M. J. *J. Am. Chem. Soc.* **1992**, *114*, 1645. (e) Cieplak, A. S.; Wiberg, K. B. *J. Am. Chem. Soc.* **1992**, *114*, 9226. (f) Wong, M. W.; Wiberg, K. B.; Frisch, M. J. *J. Am. Chem. Soc.* **1993**, *115*, 1078.
(13) Mohan, V.; Davis, M. E.; McCammon, J. A.; Pettitt, B. M. *J. Phys. Chem.* **1992**, *96*, 6428.
(14) (a) Zauhar, R. J.; Morgan, R. S. *J. Mol. Biol.* **1985**, *186*, 815. (b) Zauhar, R. J.; Morgan, R. S. *J. Comput. Chem.* **1988**, *9*, 171. (c) Zauhar, R. J.; Morgan, R. S. *J. Comput. Chem.* **1990**, *11*, 603. (d) Zauhar, R. J. *J. Comput. Chem.* **1991**, *12*, 575. (e) Fox, T.; Rösch, N.; Zauhar, R. J. *J. Comput. Chem.* **1993**, *14*, 253.
(15) (a) Warshel, A.; Russel, S. *Q. Rev. Biophys.* **1984**, *17*, 283. (b) Russel, S. T.; Warshel, A. *J. Mol. Biol.* **1985**, *185*, 389. (c) Luzhkov, V.; Warshel, A. *J. Comput. Chem.* **1992**, *13*, 199. (d) Lee, F. S.; Chu, Z. T.; Warshel, A. *J. Comput. Chem.* **1993**, *14*, 161. (e) LD/AMPAC, available from Designex, Los Angeles, CA. (f) POLARIS, available from Molecular Simulations, Inc., Burlington, MA.
(16) Ooi, T.; Oobatake, M.; Némethy, G.; Scheraga, H. A. *Proc. Natl. Acad. Sci. U.S.A.* **1987**, *84*, 3086.

0002-7863/94/1516-1502$04.50/0 

empirical solvation models have been evaluated in terms of their ability to differentiate native and near-native protein conformations.[18]

In this study, we use both microscopic and continuum solvent models for solvation studies of the diuretic drug amiloride (**1**), shown to be clinically efficacious in the treatment of hypertension, cystic fibrosis, and cancer:[19] Our chief interest is to determine

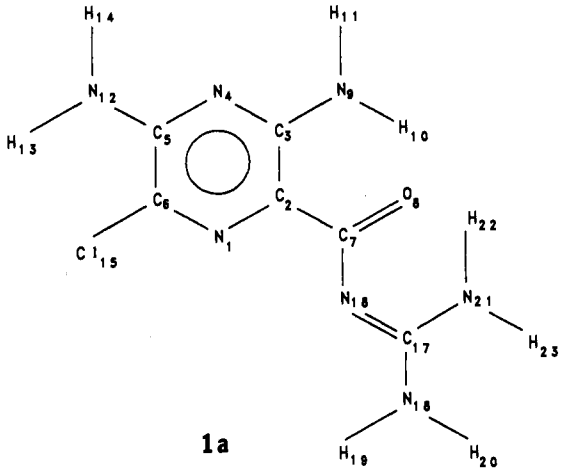


**1a**

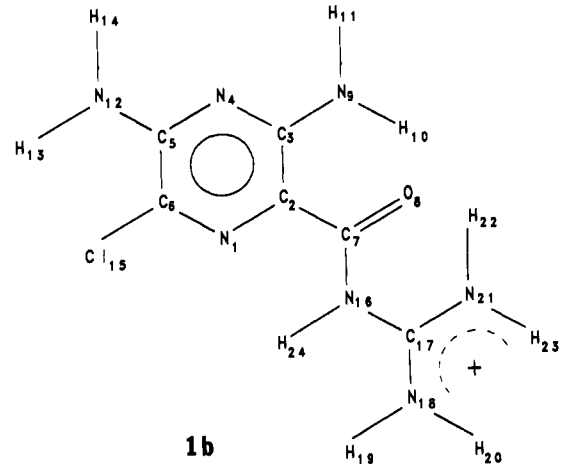


**1b**

the effect of solvation on the relative energies of the amiloride conformers in order to extend the semiempirical and NMR work of Smith et al.,[20] who were unable to unequivocally determine the solution conformation of amiloride. Few small, biologically active molecules like amiloride have been studied by molecular dynamics simulations. For example, only recently have MD simulations using explicit solvent molecules been carried out on tricyclic antidepressants[21] and small carbohydrates.[22,23] Since most empirical force fields were originally developed for proteins and nucleic acids or for simple aliphatic and aromatic compounds, extension of these force fields to new systems requires the derivation of appropriate empirical parameters.[24-27] The procedures used for deriving molecular mechanics parameters for amiloride from the results of molecular orbital calculations are described in the Methodology. Of particular interest is the torsional barrier around $-C_7-C_2-$, which determines the degree of planarity of the molecule and gives an indication of the type of low-energy binding conformations available to the molecule in its interaction with the ion channel.

In order to obtain a general indication of the relative stability of amiloride conformers in solution, we also calculate the relative hydration free energy of amiloride conformers by the induced polarization charge boundary element (IPCBE)[14] and self-consistent reaction field (SCRF)[12] continuum solvent methods and by the microscopic LD method.[15] These methods estimate the electrostatic contribution to the relative free energy of hydration but leave out other contributions such as those associated with dispersion effects. It has been previously shown that the difference in the electrostatic contribution to the hydration enthalpy and the hydration free energy is small for ions[15a,28] and for tautomeric systems.[29] We show that this is true for the amiloride conformers, as well, by using the IPCBE method to calculate the electrostatic contribution to both the hydration enthalpy and the hydration free energy for selected free base and protonated conformers.

To our knowledge, only Woodcock et al.[30] have carried out a similar comparison of continuum and microscopic models, and their study did not include the LD technique. In their analysis of tautomeric equilibria in 3- and 5-hydroxyisoxazole, as in the study of other tautomeric systems,[31] differential solvation effects calculated by the free energy perturbation technique were combined with the relative gas-phase energy differences calculated with high-level *ab initio* basis sets to predict the relative stability of tautomers in solution. The results were compared to those obtained using the SCRF technique of Tapia and Goscinski[32] and the polarizable continuum model of Tomasi and co-workers.[33]

The MD, LD, IPCBE, and SCRF techniques differ in the manner in which they treat the solvent, the solvent accessible surface and internal energy of the solute, and the effect of the solvent on the energy of the solute. The molecular dynamics method treats the solvent explicitly, which is important for studying hydrogen bonding between water and polar solutes like amiloride, but does not take into account the effect of the solvent on the electronic structure of the solute. Of the four methods studied here, only the quantum mechanical SCRF and LD/AMPAC[15c] methods incorporate the electrostatic solvent effect as an additional term in the Hamiltonian. The LD method and the IPCBE method, as originally developed[14a-d] and as used in this paper, treat the solute charge distribution as a collection of fixed point charges. However, a more exact treatment of solute charge distribution has recently been obtained by incorporation of the IPCBE method into the framework of the INDO and INDO/S-CI formalism.[14e]

The IPCBE and SCRF methods are reaction field techniques in which the solvent is treated as a continuous medium around a cavity which is defined by the molecular surface of the solute. The IPCBE method defines the cavity in a very accurate way by triangulation[14c] of the solvent accessible surface, whereas the

(17) (a) Eisenberg, D.; McLachlan, A. D. *Nature (London)* **1986**, *319*, 199. (b) Wesson, L.; Eisenberg, D. *Protein Science* **1992**, *1*, 227.
(18) Vila, J.; Williams, R. L.; Vasquez, M.; Scheraga, H. A. *Proteins: Struct., Funct., Genet.* **1991**, *10*, 199.
(19) *Amiloride and Its Analogs: Unique Cation Transport Inhibitors*; Cragoe, E. J., Jr., Kleyman, T. R., Simchowitz, L., Eds.; VCH: New York, 1992.
(20) Smith, R. L.; Cochran, D. W.; Gund, P.; Cragoe, E. J., Jr. *J. Am. Chem. Soc.* **1979**, *101*, 191.
(21) Heimstad, E.; Edvardsen, Ø.; Ferrin, T. E.; Dahl, S. G. *Eur. Neuropsychopharmacol.* **1991**, *1*, 127.
(22) Howard, E.; Grigera, J. R. *J. Chem. Soc., Faraday Trans.* **1992**, *88*, 437.
(23) (a) Brady, J. W. *Adv. Biophys. Chem.* **1991**, *1*, 155. (b) Brady, J. W. *J. Am. Chem. Soc.* **1989**, *111*, 5155.
(24) Palmö, K.; Pietilä, L. O.; Krimm, S. *Comput. Chem.* **1991**, *15*, 249.
(25) Alemán, C.; Canela, E. I.; Franco, R.; Orozco, M. *J. Comput. Chem.* **1991**, *12*, 664.
(26) Momamy, F.; Rone, R. *J. Comput. Chem.* **1992**, *13*, 888.
(27) (a) Woods, R. J.; Andrews, C. W.; Bowen, J. P. *J. Am. Chem. Soc.* **1992**, *114*, 850. (b) Bowen, J. P.; Reddy, V. V.; Patterson, D. G., Jr.; Allinger, N. L. *J. Org. Chem.* **1988**, *53*, 5471. (c) Bowen, J. P.; Pathiaseril, A.; Profeta, S., Jr.; Allinger, N. L. *J. Org. Chem.* **1987**, *52*, 5162. (d) Bowen, J. P.; Allinger, N. L. *J. Org. Chem.* **1987**, *52*, 2937.
(28) Warshel, A. *J. Phys. Chem.* **1979**, *83*, 1640.
(29) Rashin, A. *J. Phys. Chem.* **1990**, *94*, 1725.
(30) Woodcock, S.; Green, D. V. S.; Vincent, M. A.; Hillier, I. H.; Guest, M. F.; Sherwood, P. *J. Chem. Soc., Perkin Trans. 2* **1992**, 2151.
(31) Cox, J. R.; Woodcock, S.; Hillier, I. H.; Vincent, M. A. *J. Phys. Chem.* **1990**, *94*, 5499.
(32) Tapia, O.; Goscinski, O. *Mol. Phys.* **1975**, *29*, 1653.
(33) Miertuš, S.; Scrocco, E.; Tomasi, J. *Chem. Phys.* **1981**, *55*, 117.

SCRF method, in its current formalism, uses a simple sphere. In the IPCBE approach, the solute is modeled as a cavity of arbitrary shape carved out of a continuum of high dielectric constant representing the solvent. The solute charge distribution is embedded in the cavity and establishes an electric field with two components: (1) a contribution arising from the solute charges alone (calculated directly by Coulomb's law) and (2) a component due to the polarization of the solvent. This latter contribution is called the "reaction field" and depends on both the arrangement of solute charges and the specific shape of the molecule surface (dielectric boundary). In the SCRF method, the reaction field is taken to be proportional to the molecular dipole moment of the solute, with a constant of proportionality which depends on the dielectric constant of the medium. In this formalism, the reaction field, dipole moment, and correlated energy of the solute in the reaction field are determined by an iterative, self-consistent formalism.

In the LD method, the solvent system around the solute is divided into two regions. The first region is confined by a large sphere around the center of mass of the solute. The solvent molecules within this sphere are treated in a microscopic manner as polarizable point dipoles. The average polarization of the solvent dipoles is related to the corresponding local electric field in a self-consistent iterative way using the Langevin-type equation. This formula approximates the average orientational energy of the solvent molecules by an energy function that represents the average orientation of the solvent dipoles in the field of the solute charges. In the second region, the bulk solvent is treated as a continuum using the Born[1] reaction field formulas.

Although all the techniques allow for geometry optimization of the solute in the presence of the solvent, in this work, calculations (other than the MD simulations) were carried out on the same fixed molecular geometries so that the SCRF, LD, and IPCBE methods could be compared independently of differences in basis sets or force fields. In this work, these solvation techniques are applied to amiloride, a potassium-sparing acylguanidine diuretic, which, along with its analogues, has been shown to inhibit sodium transport in a variety of cellular and epithelial transport systems[34] and the mechanosensitive ion channel[35] and has been used to probe the mechanism of taste transduction.[36-39] Several recent reviews[34] have summarized the pharmacology of amiloride inhibition of ion transport systems. Since the molecular structure of the sodium channel is not known, structure–activity studies involving amiloride analogues provide a means of probing the steric and electrostatic requirements of the amiloride binding site. For example, Li et al.[40,41] have carried out a series of electrophysiological studies on the apical sodium channels of the abdominal skin of *Rana ridibunda*. These experiments relate differences in the microscopic rate constants for the binding of the analogue to alterations in the molecular structure of the pyrazine ring[40] or the acylguanidinium side chain.[41]

Knowledge of the geometry and relative energy of the conformers and tautomers of amiloride is essential to the interpretation of structure–activity data. The preferred ground-state conformers of the free base and protonated species of amiloride were determined by Smith et al.[20] using a combination of $^1H$, $^{13}C$, and $^{15}N$ NMR measurements in $Me_2SO$ and CNDO/2 semiempirical quantum mechanical calculations. Their work showed that the free base form of amiloride exists primarily in the acylimino tautomer, A (see **1a**), rather than the isoimino form, while the conjugate acid in solution is found in the F form (see **1b**). However, the authors were unable to distinguish whether the A1 ($O_8C_7C_2N_1 = 180°$) or A4 ($O_8C_7C_2N_1 = 0°$) conformer was the preferred species.

In order to interpret the activity of the amiloride analogues at the molecular level, we have initiated a molecular orbital and molecular dynamics study of the analogues tested by Li et al.[40,41] Such a comprehensive study of amiloride and its analogues could potentially be useful in the development of novel therapeutic compounds. Our work involves a multistep approach:[42] (1) molecular orbital geometry optimization to determine the structure and molecular properties of the free base[43] and protonated species of amiloride and to determine torsional barriers for molecular dynamics force field parameterization, as well as the most likely binding conformations of the protonated species; (2) *ab initio* molecular electrostatic potential (MEP) analysis[44] of analogues with pyrazine ring modifications and their complexes with the carboxylate anion, a model of the putative negative binding site on the ion channel, to determine molecular descriptors that could be useful for interpreting structure–activity data: (3) molecular dynamics simulation of amiloride in water to determine the predominant free base form in solution; (4) application of steps 1–3 to other analogues in the series with side chain modifications. Our 3-21G* geometry optimizations of rotamers of the A species[43] found the torsional barrier to be 19.0 kcal/mol, with the A1 conformer more stable by 2.50 kcal/mol than the A4. These results suggest that the A1 conformer may be the predominant free base form in solution. On the other hand, A4 has a much larger dipole moment than A1 (7.08 versus 2.68 D).[43] This indicates that solute–solvent interactions might stabilize the A4 conformation more than the A1. The present work attempts to clarify this point by calculation of the relative energies of A1 and A4 in water by means of molecular dynamics simulation and by comparison to the results of the IPCBE, LD, and SCRF calculations.

Since it is the protonated species which is active as a sodium channel blocker, we carried out an MEP analysis[44] of **1b** and related analogues with pyrazine ring modifications in order to interpret the kinetic binding data,[40] assuming that the analogues would bind to the ion channel in a planar conformation. From the MEP data, we identified the important electrostatic features that may lead to the formation of a stable analogue–channel blocking complex. The question arises, however, as to what the energetic cost might be for the protonated species to adopt nonplanar conformations. The degree of nonplanarity of amiloride is primarily determined by the height and shape of the torsional barrier around $-C_7-C_2-$. If this torsional barrier were to exhibit a broad minimum centered around the planar conformation, then it is possible that the protonated species could bind to the ion channel in a range of nonplanar conformations. In the present work we calculate the torsional barrier for F1/F4 conversion and carry out a molecular dynamics simulation of F1 in water. In

(34) (a) Garty, H.; Benos, D. J. *Physiol. Rev.* **1988**, *68*, 309. (b) Benos, D. J. In *$Na^+/H^+$ Exchange*; Grinstein, S., Ed.; CRC Press: Boca Raton, FL, 1988; p 121. (c) Kleyman, T. R.; Cragoe, E. J., Jr. In *Methods in Enzymology*; Fleischer, S., Ed.; Academic Press, New York, 1991; Vol. 191, p 739. (d) Kleyman, T. R.; Cragoe, E. J., Jr. *J. Membr. Biol.* **1988**, *105*, 1.

(35) (a) Lane, J. W.; McBride, D. W., Jr.; Hamill, O. P. *J. Physiol.* **1991**, *441*, 347. (b) Lane, J. W.; McBride, D. W., Jr.; Hamil, O. P. *Br. J. Pharmacol.* **1992**, *106*, 283.

(36) (a) DeSimone, J. A.; Heck, G. L.; De Simone, S. K. *Science* **1981**, *214*, 1039. (b) DeSimone, J. A.; Heck, G. L.; Mierson, S.; DeSimone, S. K. *J. Gen. Physiol.* **1984**, *83*, 633. (c) Heck, G. L.; Mierson, S.; DeSimone, J. A. *Science* **1984**, *223*, 403. (d) DeSimone, J. A.; Ferrell, F. *Am. Physiol. Soc.* **1985**, R52.

(37) Avenet, P.; Lindemann, B. *J. Membr. Biol.* **1988**, *105*, 245.

(38) Schiffman, S. S.; Suggs, M. S.; Cragoe, E. J., Jr.; Erickson, R. P. *Physiol. Behav.* **1990**, *47*, 455.

(39) Desor, J. A.; Finn, J. *Chem. Senses* **1989**, *14*, 793.

(40) Li, J. H.-Y.; Cragoe, E. J., Jr.; Lindemann, B. *J. Membr. Biol.* **1985**, *83*, 45.

(41) Li, J. H.-Y.; Cragoe, E. J., Jr.; Lindemann, B. *J. Membr. Biol.* **1987**, *95*, 171.

(42) Venanzi, C. A.; Venanzi, T. J. In *Mechanism of Taste Transduction*; Simon, S. A., Roper, S. D., Eds.; CRC Press: Boca Raton, FL, 1993; pp 427–462.

(43) Venanzi, C. A.; Plant, C.; Venanzi, T. J. *J. Comput. Chem.* **1991**, *12*, 850.

(44) Venanzi, C. A.; Plant, C.; Venanzi, T. J. *J. Med. Chem.* **1992**, *35*, 1643.

Table 1. Energy,[a] Dipole Moment,[b] and Geometrical Parameters[c] for Protonated Amiloride

| | $O_8C_7C_2N_1$ | | | | | | | | | | |
|---|---|---|---|---|---|---|---|---|---|---|---|
| | 180° [d] | 175° | 170° | 165° | 160° | 150° | 110° | 90° | 70° | 20° | 0° |
| $N_1C_2C_7$ | 117.8 | 117.8 | 117.8 | 117.8 | 117.8 | 117.7 | 116.4 | 116.5 | 116.8 | 111.2 | 109.9 |
| $C_7N_{16}H_{24}$ | 113.5 | 113.5 | 113.7 | 113.9 | 114.1 | 114.6 | 115.3 | 115.4 | 115.7 | 118.2 | 119.1 |
| $C_2C_3N_9$ | 123.4 | 123.4 | 123.4 | 123.5 | 123.5 | 123.6 | 123.9 | 124.1 | 124.2 | 128.0 | 129.0 |
| $C_3N_9H_{10}$ | 121.3 | 121.3 | 121.4 | 121.6 | 121.8 | 122.2 | 123.6 | 123.9 | 124.0 | 127.5 | 128.8 |
| $C_3N_9H_{11}$ | 118.2 | 118.2 | 118.1 | 118.1 | 118.1 | 118.1 | 117.7 | 117.6 | 117.4 | 115.3 | 114.7 |
| $C_6C_5H_{12}$ | 122.3 | 122.3 | 122.4 | 122.4 | 122.4 | 122.4 | 122.6 | 122.6 | 122.8 | 122.7 | 122.7 |
| $C_5N_{12}H_{13}$ | 122.9 | 122.9 | 122.9 | 122.9 | 122.9 | 122.8 | 122.6 | 122.6 | 122.5 | 122.5 | 122.5 |
| $C_5N_{12}H_{14}$ | 118.1 | 118.1 | 118.1 | 118.1 | 118.1 | 118.1 | 118.2 | 118.3 | 118.3 | 118.5 | 118.5 |
| $C_2C_7O_8$ | 126.1 | 126.1 | 126.2 | 126.2 | 126.3 | 126.6 | 128.0 | 128.2 | 128.0 | 124.5 | 123.6 |
| $O_8C_7N_{16}$ | 120.9 | 120.9 | 120.9 | 120.8 | 120.7 | 120.6 | 119.9 | 119.7 | 119.6 | 118.1 | 117.3 |
| $C_7N_{16}C_{17}$ | 126.0 | 126.0 | 126.0 | 126.0 | 126.0 | 126.0 | 126.2 | 126.2 | 125.9 | 124.9 | 124.8 |
| $N_{16}C_{17}N_{18}$ | 118.0 | 118.0 | 118.0 | 118.0 | 118.0 | 118.0 | 118.1 | 118.1 | 118.1 | 117.8 | 117.6 |
| $C_{17}N_{18}H_{19}$ | 121.7 | 121.7 | 121.7 | 121.8 | 121.8 | 121.8 | 122.0 | 122.1 | 122.1 | 122.5 | 122.7 |
| $C_{17}N_{18}H_{20}$ | 121.6 | 121.6 | 121.6 | 121.6 | 121.6 | 121.6 | 121.5 | 121.5 | 121.5 | 121.2 | 121.2 |
| $N_{16}C_{17}N_{21}$ | 120.7 | 120.7 | 120.7 | 120.7 | 120.7 | 120.7 | 120.6 | 120.6 | 120.6 | 121.2 | 121.5 |
| $C_{17}N_{21}H_{22}$ | 118.2 | 118.2 | 118.2 | 118.2 | 118.2 | 118.3 | 118.7 | 118.8 | 118.7 | 118.0 | 117.8 |
| $C_{17}N_{21}H_{23}$ | 122.0 | 122.0 | 122.0 | 122.0 | 122.0 | 121.9 | 121.9 | 121.9 | 121.9 | 121.9 | 121.9 |
| $C_7O_8$ | 1.227 | 1.227 | 1.226 | 1.225 | 1.224 | 1.222 | 1.210 | 1.207 | 1.207 | 1.212 | 1.213 |
| $C_2C_7$ | 1.429 | 1.429 | 1.431 | 1.432 | 1.434 | 1.439 | 1.469 | 2.476 | 1.470 | 1.457 | 1.461 |
| $C_3N_9$ | 1.326 | 1.326 | 1.327 | 1.327 | 1.328 | 1.330 | 1.341 | 1.345 | 1.348 | 1.352 | 1.352 |
| $C_5N_{12}$ | 1.324 | 1.324 | 1.324 | 1.324 | 1.324 | 1.325 | 1.328 | 1.329 | 1.328 | 1.324 | 1.324 |
| $C_7N_{16}$ | 1.407 | 1.407 | 1.407 | 1.408 | 1.409 | 1.411 | 1.419 | 1.422 | 1.427 | 1.428 | 1.426 |
| $N_{16}C_{17}$ | 1.345 | 1.345 | 1.345 | 1.346 | 1.346 | 1.348 | 1.352 | 1.354 | 1.355 | 1.356 | 1.357 |
| $C_{17}N_{18}$ | 1.326 | 1.326 | 1.326 | 1.325 | 1.325 | 1.325 | 1.324 | 1.324 | 1.325 | 1.328 | 1.329 |
| $C_{17}N_{21}$ | 1.312 | 1.312 | 1.312 | 1.311 | 1.311 | 1.311 | 1.310 | 1.310 | 1.309 | 1.307 | 1.306 |
| $N_9H_{10}$ | 0.998 | 0.998 | 0.998 | 0.998 | 0.997 | 0.997 | 0.995 | 0.994 | 0.994 | 0.988 | 0.986 |
| $N_9H_{11}$ | 0.999 | 0.999 | 0.998 | 0.998 | 0.998 | 0.998 | 0.998 | 0.998 | 0.999 | 1.000 | 1.000 |
| $N_{16}H_{24}$ | 1.006 | 1.006 | 1.006 | 1.005 | 1.004 | 1.003 | 1.001 | 1.001 | 1.001 | 0.993 | 0.989 |
| $N_{12}H_{13}$ | 0.997 | 0.997 | 0.997 | 0.997 | 0.997 | 0.997 | 0.996 | 0.996 | 0.996 | 0.997 | 0.997 |
| $N_{12}H_{14}$ | 0.999 | 0.999 | 0.999 | 0.999 | 0.999 | 0.999 | 0.998 | 0.998 | 0.998 | 0.999 | 0.999 |
| $N_{18}H_{19}$ | 0.999 | 0.999 | 0.999 | 0.999 | 0.999 | 0.999 | 0.999 | 0.999 | 0.999 | 0.998 | 0.998 |
| $N_{18}H_{20}$ | 0.999 | 0.999 | 0.999 | 0.999 | 0.999 | 0.999 | 1.000 | 1.000 | 1.000 | 1.000 | 1.000 |
| $N_{21}H_{22}$ | 1.009 | 1.009 | 1.009 | 1.009 | 1.009 | 1.009 | 1.008 | 1.008 | 1.008 | 1.011 | 1.011 |
| $N_{21}H_{23}$ | 0.999 | 0.999 | 0.999 | 0.999 | 0.999 | 0.999 | 0.999 | 1.000 | 1.000 | 1.000 | 1.000 |
| $H_{22}\cdots O_8$ | 1.859 | 1.859 | 1.859 | 1.859 | 1.859 | 1.860 | 1.872 | 1.870 | 1.862 | 1.804 | 1.791 |
| $H_{10}\cdots O_8$ | 2.094 | 2.099 | 2.117 | 2.146 | 2.185 | 2.290 | 2.911 | 3.202 | 3.470 | 4.232 | 4.365 |
| $H_{10}\cdots N_{16}$ | 4.024 | 4.021 | 4.016 | 4.006 | 3.992 | 3.948 | 3.570 | 3.236 | 2.863 | 2.526 | 2.596 |
| $H_{10}\cdots H_{24}$ | 4.590 | 4.585 | 4.579 | 4.565 | 4.544 | 4.480 | 3.895 | 3.404 | 2.825 | 1.730 | 1.698 |
| $H_{24}\cdots N_1$ | 2.085 | 2.090 | 2.107 | 2.134 | 2.169 | 2.258 | 2.767 | 3.065 | 3.344 | 3.872 | 3.949 |
| energy | 0.00 | 0.28 | 1.12 | 2.45 | 4.19 | 8.55 | 26.48 | 30.71 | 30.64 | 31.08 | 33.35 |
| dipole moment | 8.74 | 8.77 | 8.88 | 9.05 | 9.28 | 9.86 | 12.61 | 13.65 | 14.29 | 14.39 | 14.37 |

[a] In kilocalories/mole, relative to the conformation at $O_8C_7C_2N_1 = 180°$ (−1 141.903 365 au). [b] In debye. [c] Bond lengths in angstroms, bond angles and $O_8C_7C_2N_1$ torsional angle in degrees. [d] The energy, dipole moment, and optimized geometry at $O_8C_7C_2N_1 = 180°$ are from ref 43.

addition, the relative hydration energy of the protonated conformers is compared using the IPCBE and LD methods.

## Methodology

I. **Torsional Barrier for Protonated Amiloride.** Calculations were carried out in the 3-21G* basis set using the GAUSSIAN90[45] program at the Pittsburgh Supercomputing Center. This basis set was chosen because it has been shown to correctly predict the stability of a series of pyridone tautomers[46] and to give reliable results for molecular geometries, relative energy differences, and protonation energies for heterocyclic molecules such as pyrazine.[47] In our previous study of the free base form of amiloride,[43] we showed that the 3-21G* basis set correctly reproduced the geometry of the guanidinium side chain in the X-ray structure of 1-amidino-3-(-3-sulfamoylphenyl)urea hydrochloride.[48]

Calculations were carried out for values of the primary torsional angle, $O_8C_7C_2N_1$, equal to 175°, 170°, 165°, 160°, 150°, 110°, 90°, 70°, 20°, and 0° (F4). All bond angles and lengths were allowed to optimize except those involved in the pyrazine ring and the carbon–chlorine bond. These parameters were taken from our previous optimization[43] of the pyrazine ring model compound 2-formyl-3,5-diamino-6-chloropyrazine in the "A1-like" and "A4-like" conformations with OCCN ≈ 180° and 0°, respectively. The "A1" pyrazine ring geometry was used for optimizations with $O_8C_7C_2N_1$ between 175° and 90°; the "A4" geometry was used for optimizations with $O_8C_7C_2N_1$ less than 90°. The guanidinium side chain and amino groups were held planar in all the calculations. All torsional angles not involving these moieties were allowed to optimize. The energy, dipole moment, optimized geometry, and $-C_2-C_7-$ torsional barrier of the protonated conformers are given in Table 1.

II. **Molecular Mechanics and Dynamics.** Calculations were carried out with the GROMOS87 (GROningen MOlecular Simulation)[49a,b] package on the VAX 6430 at the New Jersey Institute of Technology. The GROMOS87 force field, developed for proteins, nucleic acids, and cyclodextrins, was altered as described below to treat the amiloride conformers.

**A. Force Field Development.** Parameter sets 1 and 2 (for the free base and protonated species, respectively) consisted of the following modifications to the GROMOS force field: (i) atomic point charges were taken from our 3-21G* molecular orbital geometry optimizations of A1 and F1 and were adjusted to conform to the GROMOS charge-group concept, (ii) Lennard–Jones $C_6$ and $C_{12}$ parameters were derived for the neutral

(45) Frisch, M. J.; Head-Gordon, M.; Trucks, G. W.; Foresman, J. B.; Schlegel, H. B.; Raghavachari, K.; Robb, M. A.; Binkley, J. S.; Gonzalez, C.; Defrees, D. J.; Fox, D. J.; Whiteside, R. A.; Seeger, R.; Melius, C. F.; Baker, J.; Martin, R. L.; Kahn, L. R.; Stewart, J. J. P.; Topiol, S.; Pople, J. A. *GAUSSIAN90*; Gaussian, Inc.: Pittsburgh, PA, 1990.

(46) (a) Schlegel, H. B.; Gund, P.; Fluder, E. *J. Am. Chem. Soc.* **1982**, *104*, 5347. (b) Scanlan, M. J.; Hillier, I. H.; MacDowell, A. A. *J. Am. Chem. Soc.* **1983**, *105*, 3568.

(47) Mo, O.; DePaz, J. L. G.; Yanez, M. *J. Mol. Struct.* **1987**, *150*, 135.

(48) Sutton, P. A.; Cody, V. *Acta Crystallogr.* **1989**, *C45*, 757.

(49) See: (a) GROMOS, developed by W. F. van Gunsteren and H. J. C. Berendsen, University of Groningen, The Netherlands. (b) van Gunsteren, W. F.; Berendsen, H. J. C.; Hermans, J.; Hol, W. G. J.; Postma, J. P. M. *Proc. Natl. Acad. Sci. U.S.A.* **1983**, *80*, 4315 and references therein. (c) GROMOS manual, available from Biomos, B. V., Groningen, The Netherlands, pp II 40–43.

**Table 2.** Atomic Point Charges for Amiloride

| | | Mulliken[a] | | PD[b] | | | | | |
|---|---|---|---|---|---|---|---|---|---|
| atom | atom type | A1 | A4 | A1 | A4 | GROMOS[c] (A1 and A4) | Mulliken[a] (F) | PD[b] (F1) | GROMOS[c] (F1) |
| $N_1$ | NR6 | −0.64 | −0.63 | −0.12 | −0.20 | −0.10 | −0.74 | 0.03 | −0.13 |
| $C_2$ | CB | 0.08 | 0.08 | −0.39 | −0.40 | 0.10 | 0.08 | −0.54 | 0.07 |
| $C_3$ | CB | 0.87 | 0.84 | 0.90 | 0.97 | 0.20 | 0.92 | 1.08 | 0.22 |
| $N_4$ | NR6 | −0.85 | −0.86 | −0.83 | −0.86 | −0.40 | −0.81 | −0.94 | −0.38 |
| $C_5$ | CB | 0.81 | 0.81 | 1.03 | 1.01 | 0.20 | 0.84 | 1.23 | 0.22 |
| $C_6$ | CB | 0.11 | 0.12 | −0.15 | −0.10 | 0.18 | 0.16 | −0.33 | 0.21 |
| $C_7$ | C | 0.90 | 0.91 | 1.15 | 1.15 | 0.35 | 0.99 | 0.78 | 0.41 |
| $O_8$ | O | −0.75 | −0.67 | −0.86 | −0.78 | −0.35 | −0.68 | −0.62 | −0.29 |
| $N_9$ | NT | −1.01 | −1.01 | −1.14 | −1.13 | −0.40 | −0.99 | −1.11 | −0.39 |
| $H_{10}$ | H | 0.41 | 0.40 | 0.52 | 0.50 | 0.22 | 0.41 | 0.49 | 0.23 |
| $H_{11}$ | H | 0.35 | 0.35 | 0.46 | 0.46 | 0.18 | 0.39 | 0.49 | 0.19 |
| $N_{12}$ | NT | −0.97 | −0.98 | −1.20 | −1.18 | −0.40 | −0.96 | −1.21 | −0.38 |
| $H_{13}$ | H | 0.38 | 0.38 | 0.47 | 0.46 | 0.20 | 0.40 | 0.50 | 0.22 |
| $H_{14}$ | H | 0.37 | 0.37 | 0.49 | 0.49 | 0.20 | 0.40 | 0.02 | 0.22 |
| $Cl_{15}$ | CL | 0.03 | 0.03 | −0.13 | −0.13 | −0.18 | 0.10 | −0.04 | −0.15 |
| $N_{16}$ | NR6 | −0.85 | −0.94 | −1.21 | −1.31 | −0.43 | −1.07 | −0.56 | −0.36 |
| $C_{17}$ | CB | 1.19 | 1.21 | 1.50 | 1.59 | 0.43 | 1.39 | 1.17 | 0.50 |
| $N_{18}$ | NT | −0.96 | −0.96 | −1.20 | −1.28 | −0.40 | −0.95 | −1.13 | −0.36 |
| $H_{19}$ | H | 0.39 | 0.37 | 0.47 | 0.50 | 0.20 | 0.41 | 0.52 | 0.24 |
| $H_{20}$ | H | 0.35 | 0.35 | 0.48 | 0.49 | 0.20 | 0.41 | 0.50 | 0.24 |
| $N_{21}$ | NT | −0.97 | −0.97 | −1.28 | −1.31 | −0.40 | −0.96 | −1.04 | −0.36 |
| $H_{22}$ | H | 0.43 | 0.44 | 0.57 | 0.59 | 0.24 | 0.46 | 0.51 | 0.30 |
| $H_{23}$ | H | 0.35 | 0.35 | 0.47 | 0.48 | 0.16 | 0.40 | 0.49 | 0.22 |
| $H_{24}$ | H | | | | | | 0.45 | 0.22 | 0.29 |

[a] 3-21G* Mulliken charges. [b] 3-21G* potential-derived charges. [c] 3-21G* Mulliken charges adjusted for GROMOS calculations as described in text.

chlorine atom, and (iii) potential functions for rotation around the $-C_2C_7-$ torsional bond were derived from our molecular orbital calculations of the $O_8C_7C_2N_1$ torsional barrier for the A and F species. These modifications are described in greater detail below.

**Atomic Point Charges.** Mulliken point charges from our 3-21G* optimization[43] of the geometries of A1 and A4 were adjusted to conform to the GROMOS charge-group concept.[49c] The nine charge groups comprising the free base forms are $N_1$–$C_2$, $C_3$–$N_4$–$C_5$, $C_6$–$Cl_{15}$, $C_7$–$O_8$, $H_{10}$–$N_9$–$H_{11}$, $H_{13}$–$N_{12}$–$H_{14}$, $N_{16}$–$C_{17}$, $H_{19}$–$N_{18}$–$H_{20}$, and $H_{22}$–$N_{21}$–$H_{23}$. These were assigned GROMOS atom types NR6–CB, CB–NR6–CB, CB–CL, C–O, H–NT–H, H–NT–H, NR6–CB, H–NT–H, and H–NT–H, respectively. Charges for F1 were assigned in the following manner in order to distribute the positive charge over the molecule. For each of the nine charge groups, the 3-21G* Mulliken charges were summed for the A1 and F1 species. The A1 sum was then subtracted from the F1 sum and the remainder was divided by the number of atoms in the charge group to give the change in charge per atom for each group. This change was then added to each of the A1 atomic charges. The charge of the F1 proton, $H_{24}$, was left at its 3-21G* Mulliken value, which is close in magnitude to that of the other adjusted GROMOS hydrogen charges. The result of this procedure is that F1 is treated as a single charge group with atomic point charges which sum to one. This procedure is in accordance with how GROMOS treats charged amino acid side chains.[49c] The 3-21G* Mulliken and adjusted GROMOS point charges are listed in Table 2.

In sections III and IV, we investigate the sensitivity of the relative hydration energy calculated by the LD and IPCBE solvent methods to the atomic point charges used in the calculation. For this reason, 3-21G* potential-derived atomic point charges were also calculated at the 3-21G*-optimized geometry for a series of free base and protonated amiloride rotamers using the Mertz–Singh–Kollman[50] option in GAUSSIAN92.[51] The charges for only the A1, A4, and F1 conformers in this series are given in Table 2. For comparison to the dipole moment calculated from the expectation value of the dipole moment operator, the dipole moment of each rotamer was calculated with these charge sets using the Quanta 3.2 software package.[52] The results are given in Table 3.

**Table 3.** Dipole Moments[a] of Amiloride Conformers

| Free Base Conformers ($O_8C_7C_2N_1$) | | | | | | |
|---|---|---|---|---|---|---|
| A1 | | | | | | A4 |
| 180° | 160° | 110° | 90° | 70° | 20° | 0° |
| 3.51[b] | 3.57 | 4.15 | 4.47 | 5.01 | 5.04 | 5.05 |
| 3.03[c] | 2.76 | 3.68 | 4.01 | 4.21 | 4.12 | 5.21 |
| 2.77[d] | 3.04 | 5.61 | 6.23 | 7.45 | 7.30 | 7.21 |
| 2.68[e] | 3.10 | 5.42 | 6.19 | 6.77 | 7.09 | 7.08 |

| Protonated Conformers ($O_8C_7C_2N_1$) | | | | | | | | | | |
|---|---|---|---|---|---|---|---|---|---|---|
| F1 | | | | | | | | | | F4 |
| 180° | 175° | 170° | 165° | 160° | 150° | 110° | 90° | 70° | 20° | 0° |
| 9.97[b] | 9.98 | 9.98 | 10.00 | 10.02 | 10.06 | 10.34 | 10.52 | 10.70 | 11.22 | 11.79 |
| 7.51[c] | 7.83 | 7.82 | 7.97 | 8.42 | 8.24 | 9.44 | 9.54 | 8.85 | 7.78 | 8.86 |
| 7.15[d] | 7.18 | 7.28 | 7.41 | 7.62 | 8.05 | 10.18 | 10.83 | 11.10 | 10.78 | 13.01 |
| 8.74[f] | 8.77 | 8.88 | 9.05 | 9.28 | 9.86 | 12.61 | 13.65 | 14.29 | 14.39 | 14.37 |

[a] In debye. [b] Using GROMOS charges from Table 2. [c] Using 3-21G* Mulliken charges, ref 43. [d] Using 3-21G* potential-derived charges, this work. [e] From the expectation value of the dipole moment operator, ref 43. [f] From the expectation value of the dipole moment operator, this work.

**Lennard–Jones Parameters for Chlorine.** Following the procedure[53] used for the derivation of other Lennard–Jones parameters in the GROMOS force field, the $C_6$ and $C_{12}$ parameters for neutral chlorine atoms were determined as follows. First, the "effective number of electrons" for chlorine was determined by a linear regression analysis of the noble gases from the data of Pitzer.[54] Calculation of linear-least-squares regression fits was performed with a program based on that of Isenhour and Jurs.[55] The slope of this regression line (with the origin included) was 0.957, yielding an effective number of electrons of 16.27 for chlorine. Second, the value of $2.18 \times 10^{-24}$ cm$^{-2}$ was used as the value for the polarizability,[56] $\alpha$, and 1.8 Å for the van der Waals radius of chlorine.[57] Finally, the Slater–Kirkwood formula[58] was used to determine the $C_6^{1/2}$ and $C_{12}^{1/2}$ parameters for chlorine. The resulting values were 48.50 (kcal·mol$^{-1}$ Å$^6$)$^{1/2}$ and 1600 (kcal·mol$^{-1}$ Å$^{12}$)$^{1/2}$, respectively.

(50) (a) Singh, U. C.; Kollman, P. A. *J. Comput. Chem.* **1984**, *5*, 129. (b) Besler, B. H.; Merz, K. M., Jr.; Kollman, P. A. *J. Comput. Chem.* **1990**, *11*, 431.

(51) Frisch, M. J.; Trucks, G. W.; Head-Gordon, M.; Gill, P. M. W.; Wong, M. W.; Foresman, J. B.; Johnson, B. G.; Schlegel, H. B.; Robb, M. A.; Replogle, E. S.; Gomperts, R.; Andres, J. L.; Raghavachari, K.; Binkley, J. S.; Gonzalez, C.; Martin, R. L.; Fox, D. J.; Defrees, D. J.; Baker, J.; Stewart, J. J. P.; Pople, J. A. *GAUSSIAN 92*, Revision A; Gaussina, Inc.: Pittsburgh, PA, 1992.

(52) *QUANTA*, Release 3.2; Polygen Corporation: Waltham, MA, July 1991.

(53) van Gunsteren, W. F. Private communication.

(54) Pitzer, K. S. *Adv. Chem. Phys.* **1959**, *2*, 59.

(55) Isenhour, T. L.; Jurs, P. C. In *Introduction to Computer Programming for Chemists: Fortran*, 2nd ed.; Allyn and Bacon, Inc.: Boston, MA, 1979; pp 160–163.

(56) Miller, T. M.; Bederson, B. *Adv. At. Mol. Phys.* **1977**, *13*, 1.

(57) In *CRC Handbook of Chemistry and Physics*, 64th ed.; Weast, R. C., Ed.; CRC Press: Boca Raton, FL, p D191.

(58) Slater, J. C.; Kirkwood, J. G. *Phys. Rev.* **1931**, *37*, 682.

**Torsional Angle Potential for X–$C_7$–$C_2$–Y.** Our *ab initio* calculations showed that the barrier to rotation around the –$C_7$–$C_2$– (GROMOS atom types C-CB) bond was 19 kcal/mol for A1/A4 and 33 kcal/mol for F1/F4 (see Table 1). The GROMOS force field, however, contained only a one-term potential function parameter for X–CB–C–Y rotation with a barrier height of 2.8 kcal/mol. For this reason, new parameters were derived using a three-term potential function to describe rotation around X–$C_7$–$C_2$–Y for both the free base and protonated species. Separate parameters were derived for the acylimino free base form (A) and for the protonated species (F). A three-step process was used to determine the potential function parameters for torsions around this important bond, which orients the side chain relative to the pyrazine ring:

(i) Using the GROMOS force field supplemented with the adjusted charges and chlorine Lennard–Jones parameters, the nonbonded energy was calculated at several values of $O_8C_7C_2N_1$ by molecular mechanics minimizations, constraining the torsional angle with an arbitrarily large force constant of 47.8 kcal/mol (200 kJ/mol).

(ii) The nonbonded energies were subtracted from the *ab initio* energies at each torsional angle value.

(iii) A three-term potential function was fit to the above energies using the method of Hopfinger and Pearlstein.[59]

For the free base and protonated species, calculations were carried out at $O_8C_7C_2N_1$ values of 0°, 20°, 70°, 90°, 110°, 160°, and 180°. For the protonated species, additional calculations were carried out at 150°, 165°, 170°, and 175°. The resulting torsional potential function parameters were $V_1 = -1.2$, $V_2 = 20.2$, and $V_3 = -1.2$ kcal/mol for the A species and $V_1 = -6.2$, $V_2 = 32.0$, and $V_3 = 6.2$ kcal/mol for the F1 species. Parameter set 1 was constructed from the standard GROMOS force field supplemented with the Lennard–Jones parameters from chlorine and the appropriate adjusted charges and primary torsional angle potential function parameters for the free base species. Set 2 was constructed as set 1, except the adjusted charges and primary torsional angle potential function parameters for the protonated species were used. Both parameter sets used the same standard GROMOS 2-fold torsional potential of 16 kcal/mol for the secondary (X–$C_7$–$N_{16}$–Y) and tertiary (X–$N_{16}$–$C_{17}$–Y) torsional angles of the side chain.

Figure 1a,b compares the potential energy surfaces of both the free base and protonated species calculated with the modified GROMOS force field and the 3-21G* basis set. The GROMOS energy was calculated at the frozen 3-21G*-optimized geometry for each conformer. Figure 1a shows that, although the molecular mechanics energy deviates from the *ab initio* energies as the primary torsional angle passes through 90° and approaches the A4 conformer, parameter set 1 gives a qualitatively correct picture of the potential energy surface of the free base species. The molecular mechanics and *ab initio* results are particularly close around the global minimum conformer (A1). Figure 1b shows that, although the molecular mechanics surface deviates from the *ab initio* surface around 0° and 20°, parameter set 2 is able to qualitatively reproduce the main features of the *ab initio* potential energy surface, especially around the global minimum conformer (F1). The deviation is caused by geometrical strain (shown in the bond stretching and angle bending terms) due to steric repulsion between $H_{10}$ and $H_{24}$.

**B. Molecular Dynamics Simulations.** The initial conformation used for the individual simulations of the A1, A4, and F1 species was the respective 3-21G*-optimized geometry.[43] All hydrogen atoms were treated explicitly. The initial conformation was first minimized until the energy change was less than 0.02 kcal/mol for the respective force field parameter set. Each solute was then solvated in a rectangular box extending 9 Å from the edges of the molecule using the SPC rigid three point charge water model.[60] The solvated system, consisting of the solute and approximately 400 water molecules, was subjected to a further round of minimization, and the resulting configuration was used as the starting point for the molecular dynamics simulations.

Molecular dynamics simulations of 30 ps in length were carried out for the A1, A4, and F1 species. After 5 ps of equilibration, data were collected from the remaining 25 ps of the trajectory. All solute bond lengths were unconstrained during the simulation. The cutoff parameter for evaluation of nonbonded interactions was set at 8 Å. Initial velocities were taken from a Maxwellian distribution at 300 K. All simulations were done at constant temperature and pressure by weakly coupling the system to a thermal bath at 300 K and a pressure bath of 1 atm. The

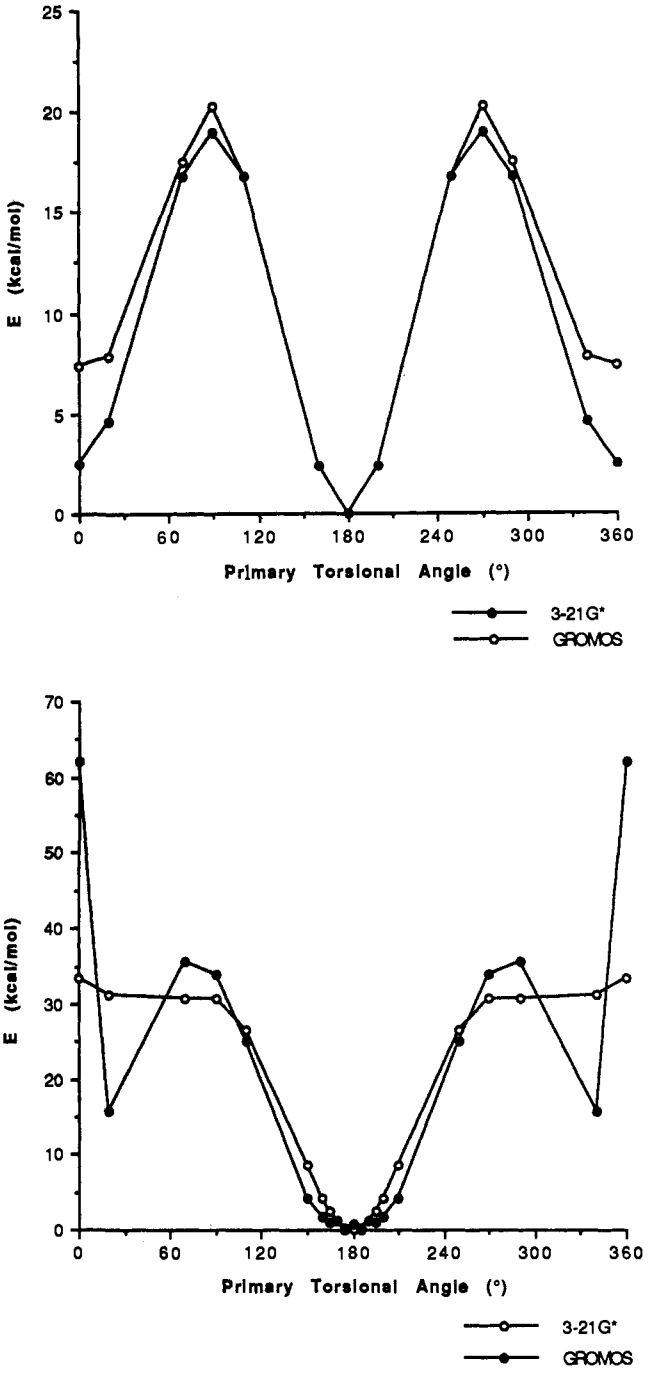


**Figure 1.** Comparison of 3-21G* and molecular mechanics rotational barriers for $O_8C_7C_2N_1$ in amiloride: (top) free base species, (bottom) protonated species.

equations of motion were integrated using a time step of 0.5 fs by applying the algorithm of Berendsen et al.[61] with a temperature relaxation time of 0.01 ps. The value of the isothermal compressibility was taken from the work of Berendsen et al.[62] Data from the trajectory was collected every 0.05 ps.

**C. Data Analysis.** The GROMOS analysis facility PROAVQ was used to calculate the average torsional angles, and PROMHB was used to calculate the data on intramolecular hydrogen bonding patterns. The averages and standard deviations of the volumes and various energy components were calculated from the GROMOS trajectory file.[63] Linear-least-squares regression fits and sample correlation coefficients of the

(59) Hopfinger, A. J.; Pearlstein, R. A. *J. Comput. Chem.* **1984**, *5*, 486.
(60) Berendsen, H. J. C.; Postma, J. P. M.; van Gunsteren, W. F.; Hermans, J., In *Intermolecular Forces*; Pullman, B., Ed.; Reidel: Dordrecht, The Netherlands; 1981; p 331–442.
(61) Berendsen, H. J. C.; Postma, J. P. M.; van Gunsteren, W. F.; DiNola, A.; Haak, J. R. *J. Chem. Phys.* **1984**, *81*, 3684.
(62) Berendsen, H. J. C.; van Gunsteren, W. F.; Zwinderman, H. R.; Geurtsen, R. G. *Ann. N. Y. Acad. Sci.* **1986**, *482*, 269.
(63) Buono, R. Unpublished program.

torsional angles were calculated by the method of Isenhour and Jurs.[55] Radial distribution functions were calculated by the method of Brunne,[64] which utilizes the half-sphere approach of Remerie.[65] Radial distribution functions for water around the side chains of the A and F species were calculated in a half sphere with the origin at $C_{17}$ and the axis defined by a line drawn between $C_{17}$ and the point which bisects the line between $N_{18}$ and $N_{21}$.

**III. Langevin Dipole Method.** The relative hydration free energy of the free base and protonated conformers of amiloride was calculated by the microscopic LD method. The positions of the solvent dipoles in the first (inner) solvation region were assigned to a cubic grid with a step of 3.1 Å. These grid points were confined by a sphere of radius 19 Å around the center of the solute. A special procedure[15c] was used to form the first solvation shell of the molecule. The dipoles were placed over the solvent accessible surface, defined by the superposition of spheres around the solute atoms with the radii equal to the sum of the water and the corresponding atomic van der Waals radii. For all the conformers of amiloride, three of the dipoles were placed at the lone pair solvation sites of atoms $N_4$, $O_8$, and $N_{16}$. The remaining part of the molecular solvation surface was equally covered with solvent dipoles with the interdipole spacing corresponding to the step of the cubic grid. This procedure resulted in an average of 30 point dipoles in the first solvation shell. The solvent dipole parameters (radius and polarizability) and the van der Waals radii of all the solute atoms except chlorine were taken from Table 1, ref 15c. A van der Waals radius of 2.0 Å was used for the chlorine atom. The dipole moment of water was taken as 1.63 D, a scaled value used to recalibrate the LD polarization to reproduce solvation free energies at room temperature.[15c] The energy of solvation was taken as an average over six different configurations of the dipole distribution over the molecular solvation surface and the corresponding outer cubic grid. The solvent in the region beyond the sphere of radius 19 Å was treated as a continuous medium with a dielectric constant of 80. The electrostatic solvation energy, $E_{elec}$, calculated by the LD method explicitly takes into account the solute interactions with the permanent and induced solvent dipoles (including mutual solute–solvent polarization) and the solvent reorganization energy.[15]

The LD model was used in two ways. First, for direct comparison with other solvent models, $E_{elec}$ was estimated for each of the conformers using the three different fixed charge sets (3-21G* Mulliken, 3-21G* potential-derived, and GROMOS). Then $\Delta E_{elec}$ was calculated as $E_{elec}(A4) - E_{elec}(A1)$ or $E_{elec}(F4) - E_{elec}(F1)$. The relative hydration free energy for A4 (F4) compared to A1 (F1), $\Delta\Delta G_{solv}$, was approximated as the sum of $\Delta E_{elec}$ and the relative energy difference of the conformers in the gas phase calculated in the 3-21G* basis set (2.5 kcal/mol for A4/A1,[43] 33.4 kcal/mol for F4/F1 (see Table 1)).

In the second approach, the solvent potential was taken into account in molecular orbital calculations using the AM1 method, in a fashion similar to that in previous MNDO calculations on other systems.[15c] In this case, $\Delta\Delta G_{solv}$ was approximated as the sum of $\Delta E_{elec}$ and $\Delta H_g^s$, where $\Delta H_g^s$ is defined as the enthalpy of formation of the solute in the gas phase. Nonplanar conformations were not studied with this approach because the AM1 method has been shown to poorly reproduce rotational barriers in conjugated molecules.[66] These two approaches thus make it possible to consider separately the effect of molecular geometry, including the accessibility of atoms to the solvent and the atomic charge distribution and the effect of amiloride electronic structure reorganization with rotation around the $-C_7-C_2-$ bond. The 3-21G*-optimized geometry was held fixed during both LD calculations. Calculations were carried out with the LD/AMPAC[15c,e] module of the POLARIS[15f] program.

**IV. Induced Polarization Charge Boundary Element Method.** For comparison with the results of the other solvation methods, calculation of the electrostatic contribution to the hydration free energies of A and F conformers was carried out using the IPCBE approach. For the free base and protonated species, the reaction field was calculated by first determining the distribution of "induced polarization charge" on the molecular solvent-accessible surface. The distributions computed for the A1 and F1 structures are illustrated in Figure 2a,b. It has been shown[67] that all of the polarization effects in a solvated system can be exactly reproduced by an appropriate distribution of induced surface charge at the dielectric boundary. For each of the amiloride conformers, the molecular surface was triangulated into collections of curvilinear finite elements using the MOLSURF package[14c] and the van der Waals radii of Rashin and Namboodiri.[68] As a test of the sensitivity of the results to the van der Waals radii used in the calculation, the relative hydration energy of A4 compared to A1 was also calculated with the GROMOS united atom radii and found to give the same result as that calculated with the Rashin and Namboodiri radii. In order to test the sensitivity of the calculations to the magnitude of the atomic point charges and to the variation of the point charges with the $O_8C_7C_2N_1$ angle, the three different atomic charge sets (3-21G* Mulliken, 3-21G* potential-derived, and GROMOS) were used to compute the distribution of the induced surface charge, which, in turn, was used to calculate the electrostatic contribution to the free energy of hydration. As with the LD method, $\Delta\Delta G_{solv}$ was approximated as the sum of $\Delta E_{elec}$ and the relative energy difference of the conformers in the gas phase calculated in the 3-21G* basis set. In all cases, a dielectric constant of 1 was used for the solute and 78 for the solvent. The computations were carried out using a range of element densities as a test of numerical convergence. It was found that a density of approximately 12 elements/Å$^2$ was sufficient to achieve numerical accuracy of better than 0.5 kcal/mol. Energy differences between conformers converged to within better than 0.2 kcal/mol.

In order to compare the relative hydration free energy calculated above to the relative hydration enthalpy of amiloride, the enthalpies of the A1,

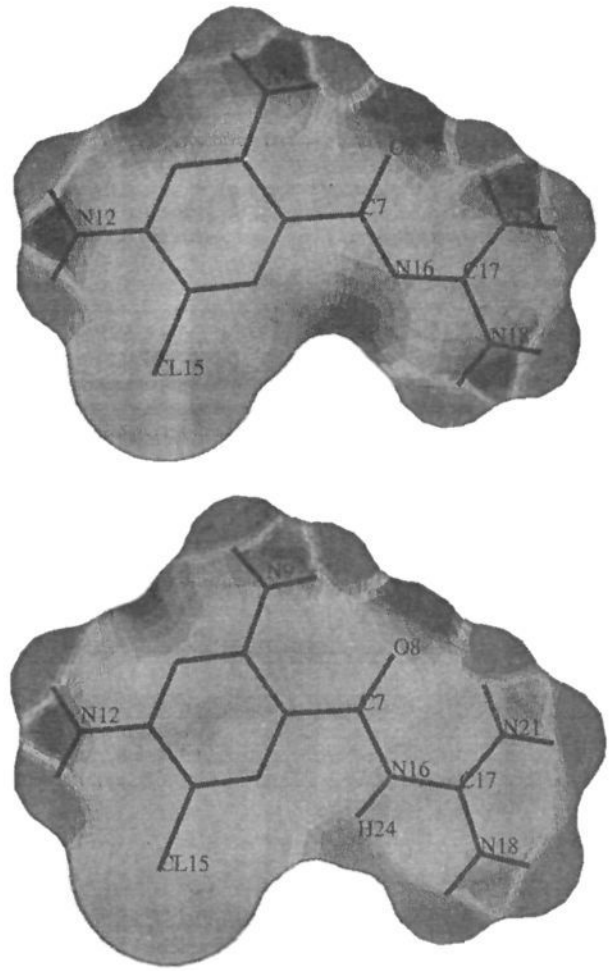


**Figure 2.** Molecular structures and associated polarization charge distributions for two of the conformers studied: (top) A1, and (bottom) F1. The distributions of polarization charge are for the potential-derived charge sets. Different shades of grey correspond to charge densities ranging from –0.015 to 0.015 e/Å$^2$, with the darker regions corresponding to charge densities of larger magnitude. The sign of the induced polarization charge is opposite to that of the corresponding atom (Table 2).

(64) Brunne, R. Unpublished program.
(65) (a) Remerie, K.; van Gunsteren, W. F.; Engberts, J. B. F. N. *Mol. Phys.* **1985**, *56*, 1393. (b) Remerie, K.; van Gunsteren, W. F.; Engberts, J. B. F. N. *Recl. Trav. Chim. Pays-Bas.* **1985**, *104*, 79.
(66) Fabian, W. M. F. *J. Comput. Chem.* **1988**, *9*, 369.
(67) Reitz, J. R.; Milford, F. J. *Foundations of Electromagnetic Theory*, 2nd ed.; Addison-Wesley: Reading, MA, 1967; p 72.
(68) Rashin, A.; Namboodiri, K. *J. Phys. Chem.* **1987**, *91*, 6003.

A4, F1, and F4 conformers were calculated by the method of Rashin and Namboodiri.[68] The temperature derivative of the solvent dielectric constant was taken as −0.3566;[69] the temperature was set at 298 K and the solvent dielectric constant at 78. The enthalpies were calculated for all three point charge sets using the Rashin and Namboodiri radii.

V. **Self-Consistent Reaction Field Method.** As a further comparison of the relative stability of the A1 and A4 conformers in solution, the SCRF method was used with the 3-21G* basis set to calculate the electrostatic contribution to the hydration free energy of the conformers at the same fixed, gas-phase, 3-21G*-optimized geometry used in the LD and IPCBE methods. Although the SCRF results are basis-set dependent and the method has only been applied to molecules smaller than amiloride and at a much higher level of theory,[12b-e] the consistent use of the 3-21G* basis set in this study provides a link between our previous gas-phase molecular orbital study and the present solvation calculations. Because the method uses a spherical cavity to define the molecular surface, the technique is most appropriately applied to small, compact molecules. However, it has been successfully applied to the study of the solvent effect on the conformational equilibrium of small, planar molecules such as furfural.[12b] Calculations were carried out using the GAUSSIAN92 package. Since the results are sensitive to the choice of cavity radius, the radius of the A1 conformer was calculated in two ways: (1) by a quantum mechanical approach which involves calculating an electron density envelope and scaling it to obtain the molecular volume[12d] or (2) from the molecular greatest dimension.[12b] The molecular greatest dimension, and therefore the cavity radius, was assumed to be the same for A1 and A4. The dielectric constant of water was taken as 78.5.

## Results

I. **Torsional Barrier and Geometrical Parameters for Protonated Amiloride.** The optimized bond angles and bond lengths are reported in Table 1 along with the relative energy and dipole moment of each conformer. The table shows that the energy of the protonated species is low between 180° and 160° (0–4.19 kcal/mol). The energy rises considerably between 150° (8.55 kcal/mol) and 110° (26.48 kcal/mol) and reaches a maximum of 33.35 kcal/mol in the F4 conformation. This can also be seen from Figure 1b. The high energy in the F4 conformer is due to steric repulsion between $H_{10}$ and $H_{24}$ and to the destabilizing effect of the large dipole moment. This indicates that the F4 conformer is unlikely to be adopted by the protonated species. However, solvent interactions may stabilize nonplanar conformers in the range of $O_8C_7C_2N_1 = 180°–160°$, and this was investigated in the molecular dynamics simulations described below.

Table 1 shows that the largest change in the bond angles occurs for those angles involved in the $O_8...H_{10}$ and $H_{24}...N_1$ hydrogen bonding patterns in F1 which are disrupted in the formation of the $H_{10}...H_{24}$ repulsion in F4. In contrast, essentially no change is seen in the angles involving the amino group at position 5 of the pyrazine ring, which is not involved in hydrogen bonding to the acylguanidinium side chain. The angles involving the carbonyl group, $C_2C_7O_8$ and $O_8C_7N_{16}$, both decrease going from F1 to F4 in response to the concomitant increase in $C_2C_7N_{16}$ due to the $H_{10}...H_{24}$ repulsion. This is also noted in the large increase in $C_7N_{16}H_{24}$ from 113.5° in F1 to 119.1° in F4. A resultant small increase is seen in $C_7N_{16}C_{17}$ from 126.0° in F1 to 128.4° in F4. The other bond angles of the guanidinium group show no significant change. The bonds which define the torsional angle go through small changes of a few hundredths of an angstrom during the change from F1 to F4. $C_7O_8$ reaches a minimum value at 90°, while $C_2C_7$ reaches a maximum at 90°. Only the NH bond lengths of those atoms involved in the repulsive $H_{10}...H_{24}$ interaction change during the rotation. The $H_{22}...O_8$ hydrogen bond distance in the side chain goes through a maximum at $O_8C_7C_2N_1 = 110°$.

Table 1 also shows a large increase in the dipole moment as the primary torsional angle changes from the F1 conformer (8.74 D) to F4 (14.37 D). This information is repeated in Table 3 to facilitate comparison with the dipole moment calculated with the 3-21G* Mulliken, 3-21G* potential-derived, and GROMOS point charges for both the free base and protonated species. The expectation value of the dipole moment operator is the most accurate value and shows the largest change going from A1 to A4 or from F1 to F4. The GROMOS calculation is the least accurate because the same set of charges is used for all the conformers of a species (see Table 2). This results in the smallest change in the dipole moment with torsional angle. However, all the methods predict A4 and F4 to have larger dipole moments than A1 and F1, respectively.

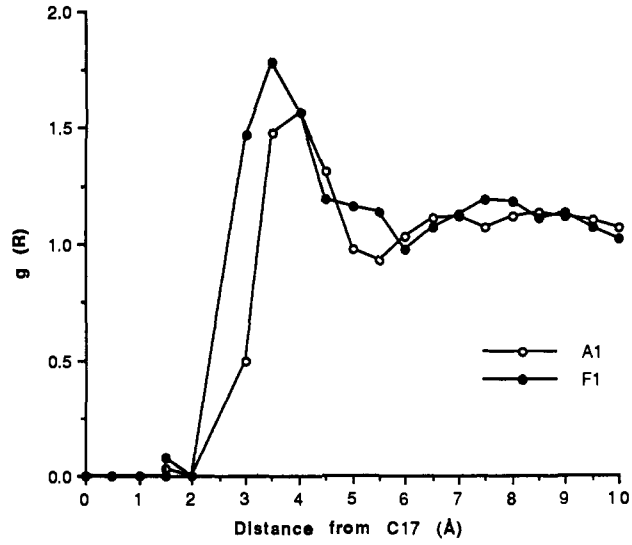


**Figure 3.** Radial distribution functions for A1 (open circles) and F1 (filled circles).

II. **Molecular Dynamics Simulations.** Figure 3 depicts the solvent radial distribution functions of the side chains of the A1 and F1 species. These results show a first solvation shell shift toward the solute of approximately 0.5 Å in the protonated form compared to the free base species, as well as a 30–50% increase in the maximum density. For the protonated species, the first maximum in the radial distribution function occurs around 3.2 Å, with a density of 1.75 molecules/Å$^3$. For the free base species, the first maximum occurs around 4.3 Å, with a density of about 1.6 molecules/Å$^3$. The minima in the radial distribution functions of the free base and protonated species occur at 5.5 and 6.0 Å, respectively.

The results of Figure 3 agree quantitatively with those of other studies. Berendsen et al.[62] found a radial distribution function of water oxygens in pancreatic trypsin inhibitor (PTI) around NZ of a Lys with a peak at 3 Å and density of 2.1 molecules/Å$^3$, which fell off sharply to 0.5 molecules/Å$^3$ at approximately 3.75 Å. This compares favorably to the amiloride simulations reported here, although in Figure 3 the radial distribution function remains around 1.0 molecules/Å$^3$ for distances larger than 5 Å. The difference in the density of water molecules around Lys compared to that around the side chain of amiloride for large values of the radius could be due to the planar structure of amiloride versus the more globular structure of PTI. Neighboring residues may block the access of water to the Lys side chain. The results shown in Figure 3 also agree qualitatively with previous analyses of experimental solvent positions around amino acids, which showed a distinct clustering occurring close to polar or charged atoms in proteins.[70]

Table 4 summarizes the average inter- and intramolecular energies from the molecular dynamics simulations. The internal energy term, $\Delta E_{int}$, shows the A1 conformer to be more stable than A4 by 3.4 kcal/mol, slightly greater than the value of 2.5 kcal/mol found by 3-21G* geometry optimization.[43] Inspection

(69) Noyes, R. M. *J. Am. Chem. Soc.* **1962**, *84*, 513.

(70) Thanki, N.; Thornton, J. M.; Goodfellow, J. M. *J. Mol. Biol.* **1988**, *202*, 637.

Table 4. Average Inter- and Intramolecular Energy,[a] Molecular Dynamics Simulations

| conformer | $V^b$ | total | kinetic | potential | water–water | internal | amiloride–water | |
|---|---|---|---|---|---|---|---|---|
| A1 | 128 ± 1 | −3399 ± 33 | 747 ± 10 | −4154 ± 35 | −4045 ± 33 | −66.8 ± 3.0 | −34.3 ± 3.4 | |
| | | | | | | | −15.9 ± 3.5[c] | |
| | | | | | | | −18.4 ± 2.0[d] | |
| A4 | 126 ± 2 | −3326 ± 29 | 735 ± 10 | −4069 ± 31 | −3962 ± 30 | −63.4 ± 2.7 | −35.7 ± 4.2 | |
| | | | | | | | −18.5 ± 4.3[c] | |
| | | | | | | | −17.2 ± 2.2[d] | |
| $\Delta E_{int}$[e] | | | | | | 3.4 | | |
| $\Delta E_{A-W}$[f] | | | | | | | −1.4 | |
| $\Delta E_{elec}$[g] | | | | | | | −2.6 | |
| $\Delta E_{LJ}$[h] | | | | | | | 1.2 | |
| $\Delta E_{tot}$[i] | | | | | | | | 2.0 |
| F1 | 127 ± 2 | −3406 ± 30 | 747 ± 11 | −4161 ± 33 | −4002 ± 32 | −53.4 ± 3.5 | −97.3 ± 7.7 | |
| | | | | | | | −83.8 ± 8.5[c] | |
| | | | | | | | −13.5 ± 3.0[d] | |

[a] In kilocalories/mole. [b] In cubic angstroms. [c] Electrostatic component ($E_{elec}$) of the amiloride–water interaction energy ($E_{A-W}$). [d] Lennard–Jones component ($E_{LJ}$) of the amiloride–water interaction energy. [e] $\Delta E_{int} = E_{internal}(A4) - E_{internal}(A1)$. [f] $\Delta E_{A-W} = E_{A-W}(A4) - E_{A-W}(A1)$. [g] $\Delta E_{elec} = E_{elec}(A4) - E_{elec}(A1)$. [h] $\Delta E_{LJ} = E_{LJ}(A4) - E_{LJ}(A1)$. [i] $\Delta E_{tot} = \Delta E_{int} + \Delta E_{A-W}$.

Table 5. Average Torsional Angles,[a] Molecular Dynamics Simulation

| | A1 | | |
|---|---|---|---|
| | set 1 | | |
| | ∠1 | ∠2 | ∠3 |
| av | −2 ± 9 | 176 ± 9 | 175 ± 10 |
| min | −42 | 146 | 149 |
| max | 26 | 199 | 209 |
| | A4 | | |
| | set 1 | | |
| | ∠1 | ∠2 | ∠3 |
| av | 175 ± 8 | 179 ± 10 | 180 ± 11 |
| min | 150 | 154 | 146 |
| max | 197 | 210 | 216 |
| | F1 | | |
| | set 2 | | |
| | ∠1 | ∠2 | ∠3 |
| av | −3 ± 11 | 177 ± 10 | −179 ± 9 |
| min | −39 | −205 | −204 |
| max | 52 | −146 | −152 |

[a] Angles in degrees: ∠1, $O_8C_7C_2N_1$; ∠2, $O_8C_7N_{16}C_{17}$; ∠3, $C_7N_{16}C_{17}N_{18}$.

of the solute–water interaction energy, $\Delta E_{A-W}$, shows that the A4–water interaction term is more favorable than the A1–water interaction term by 1.4 kcal/mol. This is due to the larger electrostatic contribution in the A4 case and is consistent with the fact that the dipole moment of the A4 conformer is larger than that of A1. However, the sum of the internal and solute–water energies, $\Delta E_{tot}$, indicates that the A1 conformer is more stable than the A4 conformer in solution by 2.0 kcal/mol.

The average torsional angles calculated for the A1, A4, and F1 conformers from the molecular dynamics simulations are summarized in Table 5. The variation of the $O_8C_7C_2N_1$ torsional angle with time is given in Figure 4a–c. The results indicate that all three conformers tend to remain planar on the average, even though nonplanar conformations are visited during the trajectory. The primary torsional angle tends to vary by ±20° from planarity for the free base species, while it varies by ±40° for F1. Correlation analyses (not shown) of the primary, secondary, and tertiary torsional angles showed that, for all combinations tested, there is no evidence of correlation between the three torsional angles.

Analysis of the intramolecular hydrogen bonding patterns in the free base and protonated species indicates that solute–solvent interactions do not significantly disrupt the intramolecular hydrogen bonding in amiloride. For the A1 conformer, the $O_8...H_{10}$ bond distance varies from 1.80 to 3.34 Å, with a median value of 2.32 Å; the $O_8...H_{22}$ bond distance varies from 1.89 to 3.63 Å, with a median value of 2.35 Å. For A4, the median $O_8...H_{22}$ bond distance is 2.33 Å and the range is 1.83–3.66 Å. For the F1 conformer, the $O_8...H_{10}$ bond distance varies from 1.86 to 3.11 Å, with a median value of 2.28 Å, and the $O_8...H_{22}$ bond distance varies from 1.76 to 3.39 Å, with a median value of 2.43 Å. The intramolecular hydrogen bonding patterns show that the median $O_8...H_{22}$ and $O_8...H_{10}$ distances from the MD simulations are somewhat larger than those of the planar *ab initio* A1, A4, and F1 conformers, which are around 1.90 Å.

**III. Langevin Dipole Method.** Table 6 shows that all the atomic point charge sets give the same qualitative pattern for the electrostatic solvation energy ($E_{elec}$) of amiloride. For both the neutral and protonated forms, the solvation energy almost steadily increases upon rotation around the $-C_7-C_2-$ bond from 180° to 0°. The solvation energy difference between the A1 and A4 or F1 and F4 conformers, $\Delta E_{elec}$, corresponds fairly well to the value of $\Delta E_{elec}$ calculated by the IPCBE method (see Table 7 and section IV below) and to the difference in the amiloride–water nonbonded interaction energy term calculated by the MD method (Table 4). The results show that the A4–water electrostatic interaction energy term is more favorable than the A1–water term, which is expected since A4 has the higher dipole moment (Table 3). The results are similar for F4 and F1. As expected, $\Delta E_{elec}$ is smallest for the GROMOS charge set due to the fact that these charges are the least polarized. However, when the difference in gas-phase internal energy is taken into account in the calculation of $\Delta\Delta G_{solv}$, the A1 conformer is calculated to be more stable than A4 in solution.

However, partitioning of $E_{elec}$ into atomic contributions (not shown) gives a complicated pattern of solute–solvent interactions that cannot be explained by a mere increase of molecular dipole moment. For the free base conformers, the greatest stabilizing effect is due to solvation of $N_{16}$ for A1 and $O_8$ for A4, i.e. atoms in the *cis* position with respect to $N_1$. In the case of the 3-21G* potential-derived charges, the solvation energy of the central $-C_7O_8N_{16}-$ group is larger for A1 than A4 by 5.7 kcal/mol. In contrast, the pyrazine ring and the guanidine moiety are more stabilized by the solvent in A4 than in A1 (by 1.7 and 5.7 kcal/mol, respectively). This could be explained by a more favorable alignment of the solvent dipoles in the electric field of these groups in the former case due to the combined effect of the changes in geometry and electronic structure upon rotation from the A1 to the A4 conformer. The difference in the electronic structures of the A1 and A4 conformers partially manifests itself in the reorientation of the molecular dipole moment by almost 90° with respect to the pyrazine ring and by the large increase in the modulus of the dipole moment. The balance between solvent

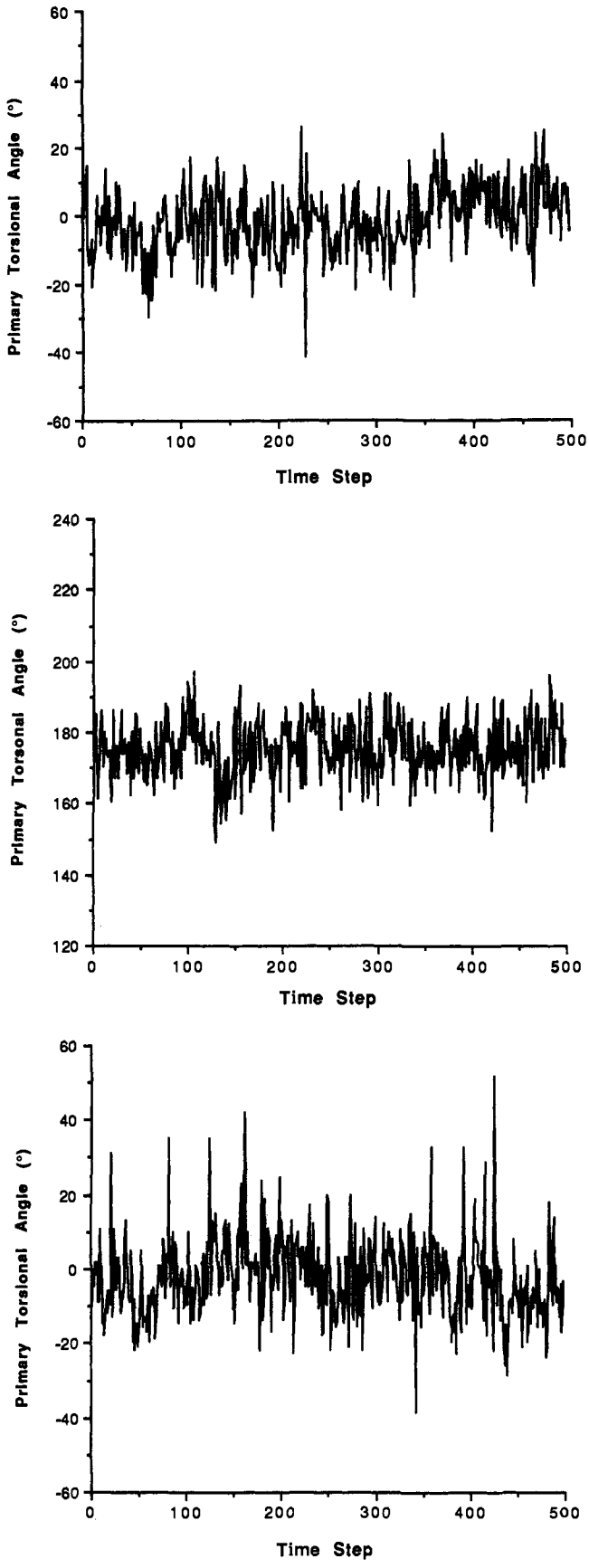


**Figure 4.** Variation in primary torsional angle ($O_8C_7C_2N_1$) with time: (a) A1, (b) A4, (c) F1.

respect to the pyrazine ring and by the large increase in the modulus of the dipole moment. The balance between solvent stabilization of different groups in this molecule leads to a greater stabilization of the A4 conformer. For the protonated conformers, the solvent stabilization is quite different from that of the free base case. Here, the largest positive charge is carried by the central carbon, $C_{17}$, of the guanidinium group (see Table 2) rather than by the atoms at the protonation site on $N_{16}$. The greater stabilization of F4 with respect to F1 is due to the more favorable solvation of the central $-C_7O_8N_{16}H-^+$ group (2.8 kcal/mol) and the remaining part of the guanidinium fragment (12.1 kcal/mol).

The difference in solvation free energies of the A1 and A4 conformers, $\Delta\Delta G_{solv}$, calculated with the LD/AM1 approach using the fixed 3-21G*-optimized geometries is also given in Table 6. The table shows that the A1 conformer is more stable than the A4 conformer by 2.1 kcal/mol. This is due to the fact that the −3.1 kcal/mol difference in the electrostatic term ($\Delta E_{elec}$) is offset by the 5.2 kcal/mol difference in the $\Delta H_g^s$ term. In addition, the LD/AM1 method takes into account the reorganization of the solute electronic structure in the field of the solvent. It is therefore more comparable to the SCRF method (see Table 8 and section V below) than either the molecular dynamics or IPCBE methods as used in this work. Comparison of the dipole moments of the isolated and solvated conformers calculated with the AM1 method shows a large difference between A1 and A4. The dipole moments of the isolated and solvated A1 are 2.2 and 2.3 D, respectively, compared to 6.2 and 10.7 D for A4. This leads to a greater stabilization of the A4 conformer due to the solute–solvent interaction compared to the fixed atomic point charge case. However, $\Delta\Delta G_{solv}$ also includes the change in the internal energy of the solute upon solvation. The balance between these terms predicts the A1 conformer to be more stable than A4 in water by 2.1 kcal/mol, in agreement with the predictions of the LD method (above) and IPCBE and SCRF methods (below) when the difference in *ab initio* gas-phase internal energy of the conformers is taken into account.

**IV. Induced Polarization Charge Boundary Element Method.** Similar to the results of the LD method, Table 7A shows that for the IPCBE method all the atomic point charge sets give qualitatively the same pattern for $E_{elec}$. Again, $E_{elec}$ almost steadily increases upon rotation around the $-C_7-C_2-$ bond from 180° to 0°. $\Delta E_{elec}$ values for A1 and A4 or F1 and F4 correspond fairly well to the LD results and to the difference in the amiloride–water interaction energy term for these conformers calculated by the MD method. For the free base conformers, $\Delta E_{elec}$ is −0.7 kcal/mol (GROMOS charge set), −1.3 kcal/mol (3-21G* Mulliken charge set), and −1.5 kcal/mol (3-21G* potential-derived charge set). With the LD method, these values are −1.1, −2.6, and −2.1 kcal/mol, respectively. From the molecular dynamics simulation (Table 4), the A4–water interaction energy is 1.4 kcal/mol more favorable than the A1–water interaction energy. For the protonated conformers, $\Delta E_{elec}$ is −4.8 kcal/mol (GROMOS charge set), −6.7 kcal/mol (3-21G* Mulliken charge set), and −17.6 kcal/mol (3-21G* potential-derived charge set) compared to the LD values of −3.3, −6.7, and −14.7 kcal/mol, respectively. As expected for a charged species, the F conformers have values of $E_{elec}$ significantly lower than the corresponding free base forms. Again, $\Delta E_{elec}$ is smallest for the GROMOS charge set. When the difference in *ab initio* gas-phase internal energy is taken into account in the calculation of $\Delta\Delta G_{solv}$, Table 7A shows that the A1 conformer is more stable than A4 in solution, in agreement with the predictions of the MD, LD, and SCRF (below) methods.

Table 7B shows that, for each point charge set, the electrostatic contribution to the relative hydration *enthalpy*, $\Delta E'_{elec}$, is quite close to the electrostatic contribution to the relative hydration *free energy*, $\Delta E_{elec}$. For the free base conformers, the values of $\Delta E_{elec}$ ($\Delta E'_{elec}$) are −0.7 (−0.8), −1.3 (−1.4), and −1.5 (−1.5) kcal/mol for the GROMOS, 3-21G* Mulliken, and 3-21G* potential-derived charges, respectively. For the protonated conformers, these values are −4.8 (−5.0), −6.7 (−7.0), and −17.6 (−18.0) kcal/

Table 6. Hydration Free Energy,[a] Langevin Dipole Method

| | Free Base Conformers ($O_8C_7C_2N_1$) | | | | | | | | |
|---|---|---|---|---|---|---|---|---|---|
| | 180° (A1) | 160° | 110° | 90° | 70° | 20° | 0° (A4) | $\Delta E_{elec}$[b] | $\Delta\Delta G_{solv}$ |
| $E_{elec}$[c] | −5.9 | −6.0 | −6.7 | −7.0 | −7.0 | −7.0 | −7.0 | −1.1 | 1.4[f] |
| $E_{elec}$[d] | −13.5 | −13.4 | −14.8 | −15.5 | −15.8 | −16.5 | −16.1 | −2.6 | −0.1[f] |
| $E_{elec}$[e] | −18.2 | −18.3 | −20.3 | −20.9 | −20.9 | −21.0 | −20.3 | −2.1 | 0.4[f] |
| $E_{elec}$[g] | −20.0 | | | | | | −23.1 | −3.1 | |
| $\Delta H_g^s$[h] | 57.4 | | | | | | 62.6 | | |
| | | | | | | | | | 2.1[i] |
| dipole[j] | 2.3 | | | | | | 10.7 | | |

| | Protonated Conformers ($O_8C_7C_2N_1$) | | | | | | | | | | | | |
|---|---|---|---|---|---|---|---|---|---|---|---|---|---|
| | 180° (F1) | 175° | 170° | 165° | 160° | 150° | 110° | 90° | 70° | 20° | 0° (F4) | $\Delta E_{elec}$[b] | $\Delta\Delta G_{solv}$ |
| $E_{elec}$[c] | −65.7 | −65.6 | −65.6 | −65.8 | −65.5 | −66.2 | −67.5 | −67.9 | −67.9 | −68.7 | −69.0 | −3.3 | 30.1[k] |
| $E_{elec}$[d] | −63.6 | −63.3 | −63.7 | −64.4 | −64.4 | −65.2 | −69.4 | −70.2 | −70.3 | −70.2 | −70.2 | −6.7 | 26.7[k] |
| $E_{elec}$[e] | −64.6 | −64.3 | −64.6 | −65.2 | −64.6 | −65.8 | −70.8 | −72.5 | −74.1 | −74.5 | −79.4 | −14.7 | 18.7[k] |

[a] In kilocalories/mole. [b] $\Delta E_{elec} = E_{elec}(A4) - E_{elec}(A1)$, or $E_{elec}(F4) - E_{elec}(F1)$. [c] Electrostatic contribution to the hydration free energy calculated with GROMOS charges from Table 2. [d] Electrostatic contribution to the hydration free energy calculated with 3-21G* Mulliken charges, ref 43 and this work. [e] Electrostatic contribution to the hydration free energy calculated with 3-21G* potential-derived charges, this work. [f] $\Delta\Delta G_{solv} = \Delta E_{elec} + E_{gas}^{3\text{-}21G*}(A4) - E_{gas}^{3\text{-}21G*}(A1) = \Delta E_{elec} + 2.50$ kcal/mol. Gas-phase relative energy difference taken from ref 43. [g] Electrostatic contribution to the hydration free energy calculated with the LD/AM1 method. [h] Enthalpy of formation of the solute in the gas phase calculated with the LD/AM1 method. [i] In the LD/AM1 method, $\Delta\Delta G_{solv} = \Delta E_{elec} + \Delta H_g^s(A4) - \Delta H_g^s(A1)$. [j] Dipole moment in the presence of solvent, in debye. [k] $\Delta\Delta G_{solv} = \Delta E_{elec} + E_g^{3\text{-}21G*}(F4) - E_g^{3\text{-}21G*}(F1) = \Delta E_{elec} + 33.4$ kcal/mol. Gas-phase relative energy difference from Table 1.

Table 7. Induced Polarization Charge Boundary Element Method

A. Hydration Free Energy[a]

| | free base conformers ($O_8C_7C_2N_1$) | | | | | | | | |
|---|---|---|---|---|---|---|---|---|---|
| | 180° (A1) | 160° | 110° | 90° | 70° | 20° | 0° (A4) | $\Delta E_{elec}$[b] | $\Delta\Delta G_{solv}$ |
| $E_{elec}$[c] | −5.7 | −5.9 | −6.5 | −6.6 | −6.5 | −6.4 | −6.4 | −0.7 | 1.8[f] |
| $E_{elec}$[d] | −17.3 | −17.2 | −17.7 | −17.7 | −17.6 | −18.4 | −18.6 | −1.3 | 1.2[f] |
| $E_{elec}$[e] | −23.9 | −24.0 | −25.2 | −25.1 | −25.3 | −24.7 | −25.4 | −1.5 | 1.0[f] |

| | protonated conformers ($O_8C_7C_2N_1$) | | | | | | | | | | | | |
|---|---|---|---|---|---|---|---|---|---|---|---|---|---|
| | 180° (F1) | 175° | 170° | 165° | 160° | 150° | 110° | 90° | 70° | 20° | 0 (F4) | $\Delta E_{elec}$[b] | $\Delta\Delta G_{solv}$ |
| $E_{elec}$[c] | −53.7 | −54.5 | −53.8 | −53.8 | −54.3 | −54.3 | −55.5 | −56.0 | −56.3 | −56.8 | −58.5 | −4.8 | 28.6[g] |
| $E_{elec}$[d] | −59.7 | −56.1 | −57.0 | −58.3 | −58.6 | −58.1 | −62.1 | −63.3 | −64.1 | −62.4 | −66.4 | −6.7 | 26.7[g] |
| $E_{elec}$[e] | −61.1 | −61.3 | −61.4 | −61.7 | −63.9 | −63.6 | −68.6 | −69.6 | −69.7 | −71.5 | −78.7 | −17.6 | 15.8[g] |

B. Hydration Enthalpy[a]

| | free base conformers ($O_8C_7C_2N_1$) | | | | protonated conformers ($O_8C_7C_2N_1$) | | | |
|---|---|---|---|---|---|---|---|---|
| | 180° (A1) | 0° (A4) | $\Delta E'_{elec}$[b] | $\Delta\Delta H_{solv}$ | 180° (F1) | 0° (F4) | $\Delta E'_{elec}$[b] | $\Delta\Delta H_{solv}$ |
| $E'_{elec}$[h] | −5.8 | −6.6 | −0.8 | 1.7[k] | −54.8 | −59.8 | −5.0 | 28.4[l] |
| $E'_{elec}$[i] | −17.8 | −19.2 | −1.4 | 1.1[k] | −60.9 | −67.9 | −7.0 | 26.4[l] |
| $E'_{elec}$[j] | −24.6 | −26.1 | −1.5 | 1.0[k] | −62.4 | −80.4 | −18.0 | 15.4[l] |

[a] In kilocalories/mole. [b] $\Delta E_{elec} = E_{elec}(A4) - E_{elec}(A1)$, or $E_{elec}(F4) - E_{elec}(F1)$. [c] Electrostatic contribution to the hydration free energy calculated with GROMOS charges from Table 2. [d] Electrostatic contribution to the hydration free energy calculated with 3-21G* Mulliken charges, ref 43. [e] Electrostatic contribution to the hydration free energy calculated with 3-21G* potential-derived charges, this work. [f] $\Delta\Delta G_{solv} = \Delta E_{elec} + E_g^{3\text{-}21G*}(A4) - E_g^{3\text{-}21G*}(A1) = \Delta E_{elec} + 2.50$ kcal/mol. Gas-phase relative energy difference from ref 43. [g] $\Delta\Delta G_{solv} = \Delta E_{elec} + E_g^{3\text{-}21G*}(F4) - E_g^{3\text{-}21G*}(F1) = \Delta E_{elec} + 33.4$ kcal/mol. Gas-phase relative energy difference from Table 1. [h] Electrostatic contribution to the hydration enthalpy calculated with GROMOS charges from Table 2. [i] Electrostatic contribution to the hydration enthalpy calculated with 3-21G* Mulliken charges, ref 43. [j] Electrostatic contribution to the hydration enthalpy calculated with 3-21G* potential-derived charges, this work. [k] $\Delta\Delta H_{solv} = \Delta E'_{elec} + E_g^{3\text{-}21G*}(A4) - E_g^{3h21G*}(A1) = \Delta E'_{elec} + 2.50$ kcal/mol. Gas-phase relative energy difference from ref 43. [l] $\Delta\Delta H_{solv} = \Delta E'_{elec} + E_g^{3h21G*}(F4) - Eg^{3\text{-}21G*}(F1) = \Delta E'_{elec} + 33.4$ kcal/mol. Gas-phase relative energy difference from Table 1.

mol. As a result, $\Delta E'_{elec}$, differs from $\Delta E_{elec}$ by a maximum of about 4% for the A1/A4 and F1/F4 amiloride conformers.

**V. Self-Consistent Reaction Field Method.** Table 8 shows the results of the SCRF method. The relative energy of A4 compared to A1, approximated by $\Delta E_{tot}$, is −1.4 kcal/mol for a cavity radius of 4.6 Å, calculated from the molecular electron density envelope, and 1.1 kcal/mol for a cavity radius of 6.2 Å, calculated from the molecular greatest dimension. This illustrates that, at least in this system, the SCRF energy is sensitive to the size of the cavity radius and that care must be taken in the choice of radius. The large discrepancy between the radii is probably due to the fact that amiloride is not a compact molecule and that a high-level basis set was not used for the calculation of the radius from the electron density envelope. The smaller radius would appear to be physically unreasonable since 4.6 Å is slightly less than one-half of the largest dimension of the molecule (5 Å). In addition, the relative energy calculated with the larger radius agrees with the general conclusions of the LD, LD/AM1, IPCBE, and MD methods in that they predict the A1 conformer to be more stable in solution than the A4 by about 1–2 kcal/mol.

The $\Delta E_{pol}$ term of the SCRF calculation is roughly comparable to the $\Delta E_{elec}$ term of the LD/AM1 calculation. The values of −1.5 kcal/mol (at radius 6.2 Å) and −5.0 kcal/mol (at radius 4.6 Å) bracket the LD/AM1 value of −3.1 kcal/mol. It is interesting to note that the MD $\Delta E_{elec}$ term, −2.6 kcal/mol, is also bracketed by the SCRF values.

Table 8 also shows that the dipole moment of the A1 conformer was found to be 3.5 D with the radius of 4.6 Å and 3.0 D with the 6.2 Å radius. For A4, these values are 9.1 and 7.8 D, respectively. This compares well to the LD/AM1 dipole moments

**Table 8.** Hydration Free Energy, SCRF Method

| | cavity radius | | | |
|---|---|---|---|---|
| | 4.6 Å | | 6.2 Å | |
| | A1 | A4 | A1 | A4 |
| $E_{pol}$[a] | −0.001411 | −0.009414 | −0.000421 | −0.002878 |
| $E_{sol}$[b] | −1141.476453 | −1141.486674 | −1141.474771 | −1141.475473 |
| $E_{tot}$[c] | −1141.475042 | −1141.477260 | −1141.474350 | −1141.472595 |
| dipole[d] | 3.5 | 9.1 | 3.0 | 7.8 |
| $\Delta E_{pol}$[e] | −5.0 | | −1.5 | |
| $\Delta E_{sol}$[f] | −6.4 | | −0.4 | |
| $\Delta E_{tot}$[g] | −1.4 | | 1.1 | |

[a] Electrostatic contribution to the hydration free energy, in hartrees. [b] Total energy of solute, in hartrees. [c] $E_{tot} = E_{sol} - E_{pol}$, in hartrees. [d] Dipole moment in the presence of solvent, in debye. [e] $\Delta E_{pol} = E_{pol}(A4) - E_{pol}(A1)$, in kcal/mol. [f] $\Delta E_{sol} = E_{sol}(A4) - E_{sol}(A1)$, in kcal/mol. [g] $\Delta E_{tot} = E_{tot}(A4) - E_{tot}(A1)$, in kcal/mol.

D (A4) in the 3-21G* basis set[43] and 2.2 (A1) and 6.2 D (A4) by the AM1 method (section III). The LD/AM1 method, therefore, predicts a larger change in the dipole moment of A4 upon solvation than does the SCRF technique.

## Conclusions

In summary, we find that the trends in $\Delta E_{elec}$ for the LD method (fixed charge model) are similar to those of the IPCBE method for both the free base and protonated conformers. In particular, for the GROMOS charge set, $\Delta E_{elec}$ calculated by the LD (−1.1 kcal/mol) and IPCBE (−0.7 kcal/mol) methods is close to the amiloride–water interaction energy term calculated in the GROMOS MD simulation (−1.4 kcal/mol). The LD/AM1 method is similar to the SCRF method in allowing polarization of the solute charge distribution. The LD/AM1 value for $\Delta E_{elec}$, −3.1 kcal/mol, falls between the SCRF $\Delta E_{pol}$ values at different cavity radii (−5.0 kcal/mol at 4.6 Å and −1.5 kcal/mol at 6.2 Å). Calculation of the electrostatic contribution to both the relative hydration enthalpy and the relative hydration free energy of amiloride conformers using the IPCBE method showed that the maximum difference in these quantities is about 4%.

The major findings of this work are as follows:

(1) Both the free base and protonated species of amiloride remain nearly planar, on the average, during the molecular dynamics simulations due to the high torsional barrier for rotation around the $-C_7-C_2-$ bond. As a result, the interaction of amiloride with discrete solvent molecules does not significantly disrupt the intramolecular hydrogen bonding pattern of **1**.

(2) All four computational methods show that the amiloride–water interaction energy is more favorable for A4 than A1, in agreement with the larger dipole moment of A4. When the difference in internal energy, which favors A1, is taken into account, all the methods predict the A1 conformer to be more stable than A4 in solution. These results help to clarify the NMR studies of Smith et al., who were not able to distinguish between A1 and A4 in solution.

(3) The qualitatively similar results of the IPCBE, LD, and SCRF methods indicate that they are practical and efficient methods for calculating the relative hydration energy for this system. The LD and IPCBE results show that, when the molecular charge distribution is given as a simple point charge approximation, the magnitude of $\Delta\Delta G_{solv}$ is more dependent on the atomic point charge set of the protonated species than of the free base species. However, the prediction of which conformer is more stable in solution is generally independent of charge set. Even though amiloride is not small and compact like other molecules which have been studied by the SCRF method, the method was nevertheless able to give results in agreement with the other methods. It has already been shown that these methods can provide a good estimate of experimental hydration enthalpies,[12,14,15,71,72] and techniques based on some of these approaches are becoming recognized as useful alternatives to carrying out molecular dynamics with explicit solvent molecules.[73] Although our results support this view, additional molecular systems should be studied in order to test the specifici applicability of the IPCBE, LD, and SCRF techniques.

(4) Surprisingly, the average MD nonbonded solute–solvent interaction energies, which neglect solvent reorganization energy, agree closely with the results of the IPCBE, LD, and SCRF methods. This approximation of relative hydration energy may prove to be a simple and useful method in studies of other pharmacologically active molecules.

(5) The planarity of the protonated species has important implications for its mode of binding to the sodium channel. Figure 1b shows that the *ab initio* energy varies little for changes in the primary torsional angle of ±20° around the F1 conformer. This indicates that F1 or conformations differing from F1 by ±20° are the most likely binding conformations. In our molecular electrostatic potential analysis of amiloride analogues with pyrazine ring substitutions at positions 5 and 6, we assumed F1 to be the binding conformation and, as a result, were able[44] to interpret kinetic data for the formation of a stable analogue–channel blocking complex in terms of the molecular electrostatic potential of the analogue. Although in the present work we studied the torsional barrier for amiloride and not for any of the analogues with pyrazine ring modifications, it is unlikely that alteration of the chlorine at position 6 to other halogens or hydrogen or the replacement of $-NH_2$ at position 5 by a chlorine would alter the torsional potential for rotation around the $-C_7C_2-$ bond. So the *ab initio* studies reported here lend support to our assumption of a planar binding conformation for this class of amiloride analogues. Presently, we are studying amiloride analogues with altered side chains. It may be that, if the ring–side chain conjugation is disrupted by an insertion of an ether oxygen or an amine group between $C_7$ and $N_{16}$, such analogues may be stable in significantly nonplanar conformations and therefore use a different mode of binding to the ion channel. Related studies are being carried out on these analogues in order to interpret the kinetic binding data[41] for this class of analogues.

**Acknowledgment.** This work was funded by grants to C.A.V. from the New Jersey Commission on Science and Technology, the Campbell Institute for Research and Technology, and the National Academy of Sciences Cooperation in Applied Science and Technology program, and by generous grants of computer time from the New Jersey Institute of Technology and the Pittsburgh Supercomputing Center. C.A.V. and T.J.V. would like to thank W. F. van Gunsteren for his hospitality during a sabbatical stay at the University of Groningen and for helpful discussions on the GROMOS force field. We would like to thank R. Brunne for making his radial distribution program available to us.

(71) Andrews, P. R.; Craik, D. J.; Martin, J. L. *J. Med. Chem.* **1984**, *27*, 1648.
(72) Lim, C.; Bashford, D.; Karplus, M. *J. Phys. Chem.* **1991**, *95*, 5610.
(73) Harvey, S. C. *Proteins* **1989**, *5*, 78.